

Disorders of the Nervous System

IgM Immunoglobulin Influences Recovery after Cervical Spinal Cord Injury by Modulating the IgG Autoantibody Response

 **Antigona Uldreaj**,^{1,2} **Pia M. Vidal**,^{1,5} **Nicole Forgiione**,¹  **James Hong**,^{1,2} and  **Michael G. Fehlings**^{1,2,3,4}

<https://doi.org/10.1523/ENEURO.0491-19.2021>

¹Division of Genetics and Development, Krembil Brain Institute, University Health Network, Toronto, Ontario M5T 2S8, Canada, ²Institute of Medical Science, Faculty of Medicine, University of Toronto, Toronto, Ontario M5T 2S8, Canada, ³Department of Surgery, Faculty of Medicine, University of Toronto, Toronto, Ontario M5T 2S8, Canada, ⁴University of Toronto Spine Program, University of Toronto, Toronto, Ontario M5T 2S8, Canada, and ⁵Department of Basic Science, Biomedical Science Research lab, Faculty of Medicine, Universidad Católica de la Santísima Concepción, Concepción, Chile 4090541

Abstract

Spinal cord injury (SCI) results in the development of detrimental autoantibodies against the lesioned spinal cord. IgM immunoglobulin maintains homeostasis against IgG-autoantibody responses, but its effect on SCI recovery remains unknown. In the present study we investigated the role of IgM immunoglobulin in influencing recovery after SCI. To this end, we induced cervical SCI at the C6/C7 level in mice that lacked secreted IgM immunoglobulin [IgM-knock-out (KO)] and their wild-type (WT) littermate controls. Overall, the absence of secretory IgM resulted in worse outcomes as compared with WT mice with SCI. At two weeks after injury, IgM-KO mice had significantly more IgG antibodies, which fixed the complement system, in the injured spinal cord parenchyma. In addition to these findings, IgM-KO mice had more parenchymal T-lymphocytes as well as CD11b+ microglia/macrophages, which co-localized with myelin. At 10 weeks after injury, IgM-KO mice showed significant impairment in neurobehavioral recovery, such as deteriorated coordination, reduced hindlimb swing speed and print area. These neurobehavioral detriments were coupled with increased lesional tissue and myelin loss. Taken together, this study provides the first evidence for the importance of IgM immunoglobulin in modulating recovery after SCI and suggests that modulating IgM could be a novel therapeutic approach to enhance recovery after SCI.

Key words: functional recovery; IgG-autoantibody response; IgM immunoglobulin; spinal cord injury

Significance Statement

The present study provides novel evidence for the protective role of IgM immunoglobulin in SCI. Using a clinically relevant mouse model of SCI at the cervical level (C6/C7), we show that deficiency of IgM immunoglobulin results in impaired neurobehavioral recovery, coupled with increased lesion size, less white matter sparing, and enhanced deposition of complement-fixing IgG antibodies in the spinal cord. These data provide evidence for the necessary role of IgM immunoglobulin in spontaneous recovery during cervical SCI and warrant more research into the therapeutic effect of IgM administration after SCI.

Received November 25, 2019; accepted June 10, 2021; First published August 19, 2021.

The authors declare no competing financial interests.

Author contributions: A.U. and M.G.F. designed research; A.U., P.M.V., N.F., and J.H. performed research; M.G.F. contributed unpublished reagents/analytic tools; A.U., P.M.V., N.F., J.H., and M.G.F. analyzed data; A.U. and M.G.F. wrote the paper.

Introduction

There is compelling preclinical and clinical evidence that spinal cord injury (SCI) results in the development of autoantibodies against spinal cord tissue as well as the induction of systemic autoantibodies (Mizrachi et al., 1983; Petrova et al., 1993; Hayes et al., 2002; Ankeny et al., 2006, 2009; Davies et al., 2007; Zajarías-Fainsod et al., 2012; Ulndreaj et al., 2017; Hergenroeder et al., 2018). Although the role of autoantibodies in human SCI remains largely unknown, research in animal models indicates that autoantibodies have a detrimental effect post-SCI (Ankeny et al., 2006, 2009). Thus, understanding the mechanisms that lead to the development of autoantibodies after SCI and limiting their detrimental effects could improve recovery in this devastating condition.

We recently found that rats with cervical SCI had an expanded IgM response, as shown by early extravasation of IgM immunoglobulin in the lesioned spinal cord and by chronically increased counts of IgM plasma cells in the spleen after injury (Ulndreaj et al., 2017). Research in other diseases suggests that IgM immunoglobulin is a key regulator of IgG-mediated autoimmunity (for review, see Ehrenstein and Notley, 2010). As such, some IgM autoantibodies have been shown to have protective effects in autoimmune conditions such as atherosclerosis and systemic lupus erythematosus (SLE). For example, increased levels of IgM autoantibodies against oxidized low-density lipoprotein (ox-LDL) and phosphorylcholine were associated with protection against atherosclerosis when adjusted for age, gender, smoking, total cholesterol levels and other factors (Su et al., 2006). Also, a lower ratio (below 0.8) of serum IgG/IgM autoantibodies against dsDNA was correlated with an absence of nephritis in patients with SLE (Förger et al., 2004). IgM immunoglobulin is also protective against infections (Boes et al., 1998a; Baumgarth et al., 2000, 2005), which are critically important in patients with SCI, as they can modulate neurologic recovery (Failli et al., 2012; Kopp et al., 2017) and constitute the most frequent co-morbidity (DeVivo et al., 1999). Lastly, IgM is the carrier and a negative regulator of apoptosis inhibitor of macrophage (AIM) protein (Hiramoto et al., 2018; Miyazaki et al., 2018). AIM, also known as CD5L/Spalpha/API6, is associated with autophagy and efferocytosis (Sanjurjo et al., 2015), and it is one of the most highly upregulated genes early on after SCI (Zhu et

al., 2017). Importantly, disruption of AIM's signaling by deletion of its receptor CD36 has been shown to result in improved neurobehavioral recovery following SCI in mice (Zhu et al., 2017).

Given this background, we posited that the expanded IgM response observed previously in our cervical SCI study could be a compensatory mechanism to limit the production of detrimental IgG autoantibodies observed post-SCI (Ulndreaj et al., 2017). Therefore, we hypothesized that mice deficient in IgM immunoglobulin will have impaired recovery after SCI. By inducing cervical SCI in a mouse model that lacks the secretory form of IgM immunoglobulin [IgM-knock-out (KO); Boes et al., 1998b], we show that lack of IgM results in the enhanced deposition of IgG antibodies in the spinal cord early on (two weeks) after injury coupled with a widespread inflammatory response in the spinal cord. Chronically (10 weeks after injury), these IgM-KO mice presented with worse locomotor recovery, increased lesion size and less white matter preservation. Thus, this study provides evidence for the protective role of IgM immunoglobulin following cervical SCI.

Materials and Methods

Mice

All animal procedures were approved by the University Health Network Animal Care Committee and experiments were conducted according to the Guide to the Care and Use of Experimental Animals designed by the Canadian Council of Animal Care. Adult female B6;129S4-Ighm^{tm1Che}/J mice were obtained from The Jackson Laboratory (JAX stock #003751; Boes et al., 1998b) and were subsequently bred at the Krembil Discovery Research Animal Facility. In these mice, the μ_s exon encoding the secreted form of the μ heavy chain, and its three downstream poly(A) sites, are replaced by the μ_m exon which encodes the constant region of the μ_4 exon and the exon encoding the membrane-bound form of IgM (Boes et al., 1998b). For this study we bred heterozygotes and used mice that were homozygous for the μ_m exon (here referred to as IgM-KO or KO) and littermate mice that were homozygous for the μ_s exon [here referred to as IgM-wild-type (WT) or WT]. As a result, the IgM-KO mice are deficient of secretory IgM immunoglobulin, although they express surface bound IgM and can class-switch into IgG immunoglobulin (Boes et al., 1998b).

C6/C7 SCI model

SCI at the C6/C7 level was induced in female adult mice as previously established in our laboratory (Forgione et al., 2017). Blood was collected via the saphenous vein from all animals 24 h before surgery to establish baseline (BSL) levels of serum immunoglobulin. To induce C6/C7 SCI, anesthesia was achieved by isoflurane (2%) delivered in a 1:1 mixture of O₂/N₂O throughout the procedure. Following skin incision and muscle retraction between C5 and T2, the C6 and C7 laminae were removed. A micro-rongeur was carefully used to widen the laminectomized area and a 5.25-g modified aneurysm clip was applied to compress the C6 level for 40 s. Next, a small piece of

This work was supported by the Paralyzed Veterans of America as well as the Gerry and Tootsie Halbert Chair in Neural Repair and Regeneration (M.G.F.).

Acknowledgements: We thank Dr. Emina Torlakovic for assessing lung inflammation in mice with SCI at two weeks after injury. Also, we thank Behzad Azad for assistance with animal care and with the Basso Mouse Scale and grip strength tests, Sadiya Yousef for assistance with animal care, Alejandro Jose for assistance with mouse breeding and ELISA protocol optimizations, and Yang Liu for assistance with mouse breeding.

Correspondence should be addressed to Michael G. Fehlings at michael.fehlings@uhn.ca.

<https://doi.org/10.1523/ENEURO.0491-19.2021>

Copyright © 2021 Ulndreaj et al.

This is an open-access article distributed under the terms of the Creative Commons Attribution 4.0 International license, which permits unrestricted use, distribution and reproduction in any medium provided that the original work is properly attributed.

Surgifoam (Ethicon) was used to cover the injured area, followed by muscle and skin suturing. Mice received subcutaneous buprenorphine (0.05 mg/kg, twice daily for 3 d) and saline (1 ml daily for 7 d) to prevent pain and dehydration, respectively. Sham mice underwent all above procedures, except for clip compression. All groups were housed in standard mouse cages (a maximum of five animals per cage), which were placed in a warm chamber of 27°C and 50% humidity. In mice with SCI, bladders were expressed manually three times a day until bladder function returned to normal. Lastly, antibiotics (Clavamox) were delivered in drinking water for two weeks to prevent infection postoperatively. Animals were sacrificed at 2 and 10 weeks after injury. The two-week study was replicated whereby two independent experimenters (A.U. and N.F.) performed surgeries, performed behavioral tests and collected tissues for subsequent analyses. Since the study cohorts showed similar neurobehavioral outcomes (data not shown) for all subsequent assessments in the study, samples were retrieved randomly from the two cohorts to minimize bias.

Behavioral analyses

Mice underwent locomotor and grip strength tests to assess their neurologic recovery at selected time points after SCI. At weeks 1–3 post-SCI, we used the Basso Mouse Scale (BMS) test and the grip strength test to assess locomotion and forelimb grip recovery, respectively (Forgione et al., 2017). For BMS testing, animals were placed individually in an open field and allowed to locomote for 5 min during which time they were scored using a previously-established 10-point scale (0–9; Basso et al., 2006). For the grip strength test, the SDI Grip Strength System model DFM-10 (San Diego Instruments) was used. In this test, forelimb motor function was assessed based on the animal's ability to pull a metal grid located on an electronic grip strength meter. Each trial consisted of five separate pulls. The highest and lowest forces were omitted and the remaining three were averaged, as previously reported (Forgione et al., 2017).

At weeks 4–10 post-SCI, we used the CatWalk XT 10.6 system (Noldus Information Technology) to assess neurologic recovery in the forelimbs and hindlimbs. Of note, the CatWalk test could not be performed before the fourth week after injury as the animals were unable to complete the test consistently. In this study, we collected a minimum of three appropriate runs per animal at 4, 8, and 10 weeks post-SCI. However, for analysis, we only considered runs demonstrating a complete gait pattern, where maximum speed variation within each run was <50%, and the average speed between runs was not significantly different (Batka et al., 2014; Vidal et al., 2017). Additionally, data from animals that were unable to perform the test reliably for reasons that were not SCI-related (such as grooming, exploring the device during the test, etc.) were not collected for analysis. The parameters selected for analysis were stride length, print area, swing speed, swing time, step sequence regularity and average body speed, as previously reported (Forgione et al., 2017). All above tests were performed by one experimenter who was blinded to the groups.

Tissue collection and processing

At 2 and 10 weeks after injury, animals received an overdose of inhalant isoflurane and tissues were collected in the following order. Blood was collected from the heart and was left to clot at room temperature (RT) for at least 30 min for serum preparation for ELISA to confirm the absence of secretory IgM in KO mice and for the quantification of serum IgG and IgM. Next, animals were transcardially perfused with ice-cold PBS followed by isolation and processing of tissues of interest.

The bladder and a piece of the colon from each animal were weighed, homogenized in sterile PBS, serially diluted and then cultured in standard LB agar plates for 24 h at 37°C. The lungs were fixed in 4% paraformaldehyde (PFA) for 30 min and then in formalin overnight, followed by embedding, sectioning and staining for histology assessment as previously described (Uldreaj et al., 2017). Spinal cords were fixed in 4% PFA-PBS for 3 h, then incubated in 10% sucrose (w/v)-PFA for 3 h, followed by an overnight incubation in 20% sucrose (w/v)-PBS at 4°C. A 1-cm-long section of the cervical cord centered at the injury epicenter was further selected for sectioning and 30- μ m-thick cryosections were stored at -80°C before use for immunofluorescence staining.

Quantitative lesion analysis

Lesion analysis was performed at 2 and 10 weeks post-SCI. Thirty-micrometer-thick sections at 600- μ m intervals were stained with luxol fast blue (LFB) and hematoxylin-eosin (HE). Stereology was conducted using a Nikon Eclipse E800 microscope with a motorized stage and StereoInvestigator software (MBF Biosciences). Lesion volume and spared gray/white matter volume were quantified for each section using the Cavalieri Estimator function. Spared gray matter was considered as the non LFB-stained area displaying normal cytoarchitecture and easily distinguishable neuronal cell bodies. Spared white matter was considered as the LFB-stained area with normal architecture and non-lesional tissue. As previously reported (Forgione et al., 2017), here we defined lesional tissue as areas with loss of normal cytoarchitecture, absence of neuronal cell bodies, presence of fibrotic and/or glial scar tissue, infiltrated immune cells, as well as presence of vacuoles and loss of LFB stain (in gray matter).

Immunofluorescence assessments in the lesioned spinal cord

IgG deposition in the injured spinal cord

IgG deposition in the lesioned spinal cord was assessed by quantifying the % area of IgG+ immunofluorescent signal at 2 and 10 weeks post-SCI, following a previously reported protocol (Uldreaj et al., 2017). Of note, this method is not sensitive to the intensity of the detected signal, but rather it semi-quantifies the spread of the IgG content on the tissue. Thus, IgG deposition refers to the degree of IgG spread on the tissue, expressed as percent of the total spinal cord section.

In brief, following air-drying and rehydration in PBS, cryosections were blocked with 5% goat serum + 1%

BSA + 0.3% Triton X-100 in PBS for 1 h at RT. Cy3-conjugated goat anti-mouse F(ab')₂ IgG antibody (1:250, Jackson ImmunoResearch) and 4',6-diamidino-2-phenylindole (DAPI; 1:250) were added to the slides and incubated overnight at 4°C. Of note, a F(ab')₂ IgG detecting antibody was used to minimize labeling of Fc receptors in the injured parenchyma. Sections were washed four times with PBS and slides were cover-slipped with Mowiol mounting medium (Sigma). To avoid staining variability, all samples from the same time point were stained simultaneously.

Samples were selected randomly for imaging and images were acquired as close together as possible. For the two-week time point, a Nikon Eclipse E800 microscope at 10× magnification was used. The threshold was set such that the brightest sections (injury epicenter) were not overexposed yet signal from the least bright sections could still be detected. A similar procedure, although using a Nikon eclipse Ti C2+ inverted confocal microscope, was followed for the 10-week time point. At both time points, all settings were kept constant during imaging. Signal from spinal cord sections, excluding the dura, was measured with the appropriate plugin in ImageJ software and assessed under identical settings. The IgG+ area was expressed as % of the total area of the spinal cord section.

Complement-fixing IgGs

Complement fixation by deposited IgGs in the spinal cord was assessed in spinal cord sections with the highest IgG signal. These sections, which were located -1200, -600, and +600 μm from the injury epicenter, were co-stained for IgG and complement C3b protein and the amount of complement fixing IgGs was semi-quantified based on the IgG+/C3b+ positive immunofluorescent area. Briefly, sections were first stained for IgG as described above. Next, they were incubated with anti-mouse C3b-FITC antibody (1:100, Cederlane, clone 11H9 recognizing C3/C3b/iC3b) and DAPI (1:250) diluted in 5% goat serum + 1% BSA + 0.3% Triton X-100 in PBS, overnight at 4°C. Lastly, sections were washed, cover-slipped and imaged with a Nikon eclipse Ti C2+ inverted confocal microscope, as described above. For each section, the area of positive immunofluorescence from IgG alone, C3b alone and IgG and C3b signal was estimated with ImageJ and expressed as % of the total area of the spinal cord section. Then, the obtained values for the three sections (representing distances -1200, -600, and +600 μm from the injury epicenter) were averaged per animal.

Serum IgG and IgM immunoglobulin levels

Serum IgG and IgM immunoglobulin was quantified by ELISA developed in-house. Briefly, standard 96-well plates were coated with 2 μg/ml of either capturing anti-mouse IgG antibody (Abcam) or anti-mouse IgM antibody (Abcam, ab 9175) O/N at 4°C. Following one wash with PBS, plates were blocked with 4% goat serum in PBS for 2 h at RT. Next, serum diluted in 4% goat serum was added at 1:50,000 (for detection of IgG) and at 1:10,000 (for detection of IgM) and incubated for 4 h at RT. Mouse

IgG (Sigma, 15381) or IgM (BioLegend, 401601, clone MM-30) purified from mouse serum was serially diluted in 1:2, starting from 10 μg/ml, to create a standard curve in every plate ranging from 10 μg/ml to 9.8 ng/ml. Plates were then washed with 0.05% Tween in PBS and incubated for 30 min at RT with anti-mouse IgG-HRP (Sigma) or IgM-HRP (Abcam) antibody diluted 1:10,000 in 4% goat serum. Following four washes, plates were incubated with UltraFast TMB ELISA substrate (ThermoFisher Scientific) followed by deactivation of the chromogenic reaction with sulfuric acid (2 M, Sigma). Samples and standards were run in duplicates. IgG and IgM concentration in serum was interpolated from the standard curve to which a 4PL nonlinear curve fit was applied using Prism (GraphPad) software.

T-lymphocytes and microglia/macrophages

T-lymphocyte infiltration and microglia/macrophages in the spinal cords of IgM-KO and WT mice were assessed by immunohistochemistry IHC at 2 and 10 weeks post-SCI in 11 sections per animal at 600-μm intervals.

For IHC staining, sections were first blocked in 5% goat serum + 1% BSA + 0.3% Triton X-100 in PBS. Next, sections were incubated with primary antibodies against the T-cell marker CD3 (goat anti-mouse CD3, 1:1000, Alexa Fluor 568, BioLegend) or the macrophage marker CD11b (rat anti-mouse CD11b, 1:300, Millipore CBL1313) overnight at 4°C. DAPI (1:250) was incubated with the anti-CD3 primary antibody or with the secondary antibody in sections stained for CD11b (goat anti-rat IgG, 1:500, Alexa Fluor 488, Life technologies), also overnight at 4°C.

Following imaging with a Nikon Eclipse E800 microscope at 10× magnifications, CD3+ or CD11b+ immunofluorescent areas or cell counts were estimated by ImageJ.

Myelin-engulfing macrophages

Myelin-engulfing macrophages were assessed in sections with the most intense IgG deposition (-1200, -600, and +600 μm from the injury epicenter). To this end, the selected sections were co-stained for fluoromyelin and CD11b. First, sections were stained for CD11b (primary + secondary antibody) as described above. Next, following washes, sections were incubated with fluoromyelin (1:100, Life Technologies, F34652) and DAPI (1:250) in 5% goat serum + 1% BSA + 0.3% Triton X-100 in PBS, overnight. Images were acquired with a Nikon eclipse Ti C2+ inverted confocal microscope under identical settings for each marker. The area of positive immunofluorescence for each marker was estimated with ImageJ and expressed as % of the total DAPI+ area of the spinal cord section. Here, we report averaged values that were obtained from three sections (representing distances -1200, -600, and +600 μm from the injury epicenter) per animal.

Experimental design and statistical analysis

Sample sizes for all experiments in this study were determined a priori based on previous studies with similar animal models and experimental design (Forgione et al., 2017; Uldreaj et al., 2017). Considering the predefined

sample size, samples that were assessed were selected randomly from the pool of all samples collected. All experimental assessments, data collection and analyses were performed by experimenters who were blinded to the study groups. All ImageJ analyses were performed in an automated fashion to minimize human bias.

Prism (GraphPad) and SPSS (IBM) were used for hypothesis-testing statistical analyses of all the data. Comparisons between two groups were conducted using Student's *t* tests for parametric data, and Mann-Whitney tests for non-parametric data. Statistical comparisons for more than two groups were conducted with one-way ANOVA and Bonferroni *post hoc* tests for parametric data or with Kruskal-Wallis tests for non-parametric data, respectively. All tests were two-tailed and statistically significant differences were considered to be those with a $p \leq 0.05$. CatWalk data were first analyzed by repeated measures to reveal changes between groups over time (Table 1). Parameters that were shown by repeated measures tests to differ significantly between groups were further analyzed by one-way ANOVA and Bonferroni *post hoc* tests to compare groups within each time point. Results are shown as individual data points, with each data point representing one animal. Bars indicate mean \pm standard error of the mean (SEM) unless otherwise specified. Results from hypothesis testing statistical analyses are reported in the statistical table (Table 1).

Where possible, estimation statistical analyses reporting effect size, confidence intervals (CIs) and *p* values of permutation *t* tests, were performed according to (Ho et al., 2019) using the online tool (<https://www.estimationstats.com>). Briefly for these analyses, 5000 bootstrap samples were taken, and the CI was bias-corrected and accelerated. For each permutation *p* value, 5000 reshuffles of the control and test labels were performed. The *p* values reported are the likelihood of observing the corresponding effect size, if the null hypothesis of zero difference is true. In this study, statistical significance of the permutation *p* value was set to 0.05 and therefore, in the graphs of data where permutation *p* values were <0.05 , the significant difference is indicated accordingly with asterisks (Figs. 1E-I, 3E, 5A,C-H, 6B-E). Table 2 summarizes the effect size (unpaired mean difference) of the difference between compared groups and the 95% CI with lower and upper bound, as well as the *p* values of permutation tests. Gardner-Altman estimation plots were generated using the online tool (<https://www.estimationstats.com>) where possible (Figs. 1E-I, 3E, 5A, 6B-E). Such plots depict the compared groups and the mean difference between the groups as a bootstrap sampling distribution. The mean difference is depicted as a dot; the 95% CI is indicated by the ends of the vertical error bar. Of note, CatWalk data were analyzed by both types of statistical approaches. Three-way ANOVA with *post hoc* test was performed to look at the effect of genotype, time point and injury status on the selected CatWalk parameters (Table 1), whereas estimation statistics were used to compare the WT-SCI and KO-SCI only, within each time point.

CatWalk data were not graphed as Gardner-Altman plots for aesthetic reasons. Asterisks on the graphs representing CatWalk data refer to significant results from estimation statistics comparing WT-SCI and KO-SCI within each time point of the study (Table 2).

Results

IgM-KO mice show increased deposition of complement-fixing IgG antibodies

Antibodies accumulate in the injured parenchyma during the subacute phase of cervical SCI in rats (Ulndreaj et al., 2017) and during the chronic phase of thoracic SCI in mice (Ankeny et al., 2009). Such antibodies have been shown to be autoreactive (Ankeny et al., 2006, 2009; Ulndreaj et al., 2017) and pathogenic by activating the classical complement system pathway (Ankeny et al., 2009). As IgM has been shown to regulate IgG autoimmunity under normal conditions (Boes et al., 2000), we hypothesized that IgM-KO mice would have increased IgG-antibody deposition in the lesioned spinal cord during the subacute phase of our cervical SCI model, compared with their WT counterparts.

In line with this hypothesis, we found enhanced IgG deposition in IgM-KO mice, as shown by increased % area of IgG+ immunofluorescence compared with WT mice (Fig. 1A,B; Table 1). Particularly at distances -1200 , -600 , and $+600 \mu\text{m}$ from the injury epicenter, the deposited IgG was $\sim 125\%$ higher in KO mice than in the WT group. However, the enhanced antibody accumulation did not appear to be sustained in the chronic phase of injury, as there was no significant difference in % IgG+ immunofluorescent area between injured IgM-KO and WT mice at 10 weeks post-SCI (Fig. 1C; Table 1).

To establish whether the IgG deposited in the spinal cord after injury could activate the complement system, we selected sections with the highest IgG accumulation (e.g., at distances -1200 , -600 , and $+600 \mu\text{m}$ from the injury epicenter) and co-stained them for IgG and complement C3b protein (Fig. 1D). As expected, there was increased IgG deposition in IgM-KO mice in comparison to controls (Fig. 1E; Table 2). Moreover, the IgG-C3b co-stained area was significantly larger in IgM-KO mice than in WT controls with SCI, indicating enhanced complement-fixing activity of deposited IgG in the spinal cord of KO mice (Fig. 1F; Table 2). However, C3b deposition alone was not significantly different between IgM-KO mice and WT controls with SCI (Fig. 1G; Table 2) suggesting that lack of IgM does not affect complement deposition through all pathways, but rather complement deposition through the classical (antibody-mediated) pathway. Of note, one cannot exclude the possibility that lack of statistical difference (effect size 12.5, 95%CI: 1.48, 23.1, permutation $p=0.116$; Table 2) between the groups in Figure 1G could be because of increased variance in the WT samples.

To exclude Fc-mediated binding of the labeling anti-C3b antibody in the spinal cord, in our optimization assays we used a mix of Fc blocking peptides (Innovex,

Table 1: Hypothesis testing statistics table showing the statistical tests used in the study and respective results

Figure	Panel	Measure	Groups (sample size)	Test	Details	Statistic	p value	
1	B	Effect of secretory IgM on the % area of IgG deposition at 2 weeks post-SCI	KO (4), WT (5) mice	Two-way ANOVA Sidak's <i>post hoc</i> to compare between KO and WT mice for each distance point Factor 1 (genotype), factor 2 (distance from epileft)	Effect of genotype	$F = 21.31$	<0.0001	
					Section -1200 μm	$t = 3.528$	0.0078	
					Section -600 μm	$t = 3.513$	0.0082	
	C	Effect of secretory IgM on the % area of IgG deposition at 10 weeks post-SCI	KO (4), WT (4) mice	Two-way ANOVA Factor 1 (genotype), factor 2 (distance from epileft)	Effect of genotype	$F = 1.965$	0.1657	
					Section 600 μm	$t = 2.957$	0.0445	
	H	Effects of secretory IgM on levels of serum IgG immunoglobulin	KO: BSL (9), 2 weeks (5), 10 weeks (7) mice WT: BSL (10), 2 weeks (6), 10 weeks (6) mice	One-way ANOVA Holm-Sidak's multiple comparisons test	One-way ANOVA be-	$F = 6.694$	0.0002	
					tween WT and KO			
					BSL: (KO vs WT)	$t = 0.760$	0.6995	
					2 weeks post-SCI: (KO vs WT)	$t = 1.950$	0.1662	
					10 weeks post-SCI: (KO vs WT)	$t = 0.330$	0.7431	
2	B	Effect of secretory IgM on the % area of CD3+ cell infiltration at 2 weeks post-SCI	KO (4), WT (5) mice	Two-way ANOVA Sidak's <i>post hoc</i> to compare between KO and WT mice for each distance point Factor 1 (genotype), factor 2 (distance from epileft)	Effect of genotype	$F = 15.93$	0.0001	
					Section -1200 μm	$t = 2.689$	0.0088	
					Section -600 μm	$t = 2.862$	0.0054	
					Section 0	$t = 2.29$	0.0248	
	C	Effect of secretory IgM on CD3+ cell counts at 2 weeks post-SCI	KO (5), WT (5) mice	Two-way ANOVA Sidak's <i>post hoc</i> to compare between KO and WT mice for each distance point Factor 1 (genotype), factor 2 (distance from epileft)	Effect of genotype	$F = 9.394$	0.0029	
					Section -1200 μm	$t = 2.000$	0.0486	
	C	Effect of secretory IgM on CD3+ cell counts at 10 weeks post-SCI	KO (5), WT (5) mice	Two-way ANOVA Sidak's <i>post hoc</i> to compare between KO and WT mice for each distance point Factor 1 (genotype), factor 2 (distance from epileft)	Section -600 μm	$t = 2.095$	0.039	
					Section 0	$t = 2.275$	0.0253	
					Section 600 μm	$t = 2.483$	0.0149	
					Effect of genotype	$F = 7.335$	0.0081	
3	B	Effect of secretory IgM on the % area of CD11b+ cells at 2 weeks post-SCI	KO (4), WT (5) mice	Two-way ANOVA Sidak's <i>post hoc</i> to compare between KO and WT mice for each distance point Factor 1 (genotype), factor 2 (distance from epileft)	Effect of genotype	$F = 20.69$	<0.0001	
					Section -1200 μm	$t = 2.471$	0.0157	
					Section 0	$t = 3.031$	0.0033	
					Section 600 μm	$t = 2.800$	0.0065	
	C	Effect of secretory IgM on CD11b+ cell counts at 2 weeks post-SCI	KO (5), WT (5) mice	Two-way ANOVA Sidak's <i>post hoc</i> to compare between KO and WT mice for each distance point Factor 1 (genotype), factor 2 (distance from epileft)	Effect of genotype	$F = 21.61$	<0.0001	
					Section -1200 μm	$t = 2.096$	0.039	
	C	Effect of secretory IgM on CD11b+ cell counts at 10 weeks post-SCI	KO (5), WT (5) mice	Two-way ANOVA Sidak's <i>post hoc</i> to compare between KO and WT mice for each distance point Factor 1 (genotype), factor 2 (distance from epileft)	Section 600 μm	$t = 2.566$	0.012	
					Effect of genotype	$F = 21.92$	<0.0001	
					Section -2400 μm	$t = 2.573$	0.0117	
					Section -1200 μm	$t = 2.421$	0.0175	
C	Effect of secretory IgM on CD11b+ cell counts at 10 weeks post-SCI	KO (5), WT (5) mice	Two-way ANOVA Sidak's <i>post hoc</i> to compare between KO and WT mice for each distance point Factor 1 (genotype), factor 2 (distance from epileft)	Section -600 μm	$t = 2.647$	0.0096		
				Section 1200 μm	$t = 2.074$	0.041		

(Continued)

Table 1: Continued

Figure	Panel	Measure	Groups (sample size)	Test	Details	Statistic	p value	
4	B	Effect of secretory IgM on % lesional tissue at 2 weeks post-SCI	KO (4), WT (5) mice	Two-way ANOVA Factor 1 (genotype), factor 2 (distance from epilept)	Effect of genotype	F = 2.681	0.1056	
	C	Effect of secretory IgM on % white matter preservation at 2 weeks post-SCI	KO (4), WT (5) mice	Two-way ANOVA Factor 1 (genotype), factor 2 (distance from epilept)	Effect of genotype	F = 0.199	0.6566	
	D	Effect of secretory IgM on % gray matter preservation at 2 weeks post-SCI	KO (4), WT (5) mice	Two-way ANOVA Fisher's <i>post hoc</i> to compare between KO and WT mice for each distance point Factor 1 (genotype), factor 2 (distance from epilept)	Effect of genotype	F = 6.544	0.0061	
	E	Effect of secretory IgM on % lesional tissue at 10 weeks post-SCI	KO (4), WT (5) mice	Two-way ANOVA Fisher's <i>post hoc</i> to compare between KO and WT mice for each distance point Factor 1 (genotype), factor 2 (distance from epilept)	Section 0 Effect of genotype	t = 2.817 F = 22.53	0.0062 < 0.0001	
					Section -2400 μm Section -1200 μm Section -600 μm	t = 2.041 t = 2.216 t = 3.328	0.0452 0.0302 0.0014	
4	F	Effect of secretory IgM on % white matter preservation at 10 weeks post-SCI	KO (4), WT (5) mice	Two-way ANOVA Fisher's <i>post hoc</i> to compare between KO and WT mice for each distance point Factor 1 (genotype), factor 2 (distance from epilept)	Effect of genotype	F = 33.38	< 0.0001	
					Section -2400 μm Section -1200 μm Section -60 μm	t = 2.579 t = 2.574 t = 2.918	0.0121 0.0123 0.0048	
					Section 1800 μm Section 2400 μm Section 3000 μm	t = 2.496 t = 2.331 t = 2.028	0.0151 0.0228 0.0466	
	G	Effect of secretory IgM on the % gray matter preservation at 10 weeks post-SCI	KO (4), WT (5) mice	Two-way ANOVA Factor 1 (genotype), factor 2 (distance from epilept)	Effect of genotype	F = 0.1437	0.7059	
	5	C	Effect of secretory IgM on step sequence regularity at 4, 8, and 10 weeks post-SCI		Three-way ANOVA One-way ANOVA for groups within each time point Sidak's multiple comparisons <i>post hoc</i> test on one-way ANOVA Factor 1 (genotype), factor 2 (injury status), factor 3 (time post-SCI)	Effect of genotype × injury	F = 10.23	0.0019
				4 weeks: KO SCI (10), KO sham (10) WT SCI (7), WT sham (10) mice		4 weeks one-way ANOVA KO SCI vs KO sham KO SCI vs WT SCI WT SCI vs WT sham	F = 9.625 t = 3.985 t = 0.427 t = 3.468	0.0001 0.0011 0.9648 0.0044
				8 weeks: KO SCI (10), KO sham (8), WT SCI (7), WT sham (9) mice		8 weeks one-way ANOVA KO SCI vs KO sham KO SCI vs WT SCI WT SCI vs WT sham	F = 36.14 t = 36.14 t = 3.675 t = 4.362	< 0.0001 < 0.0001 0.0028 0.0004
			10 weeks: KO SCI (7), KO sham (8), WT SCI (6), WT sham (8) mice		10 weeks one-way ANOVA KO SCI vs KO sham KO SCI vs WT SCI WT SCI vs WT sham	F = 28.85 t = 8.244 t = 4.415 t = 3.065	< 0.0001 < 0.0001 0.0005 0.0154	
D		Effect of secretory IgM on hindlimb swing speed at 4, 8, and 10 weeks post-SCI		Three-way ANOVA One-way ANOVA for groups within each time point Sidak's multiple comparisons <i>post hoc</i> test on one-way ANOVA Factor 1 (genotype), factor 2 (injury status), factor 3 (time post-SCI)	Effect of genotype × injury	F = 5.351	0.0229	
			4 weeks: KO SCI (10), KO sham (10) WT SCI (7), WT sham (10) mice		4 weeks one-way ANOVA KO SCI vs KO sham KO SCI vs WT SCI WT SCI vs WT sham	F = 2.606 t = 2.535 t = 1.015 t = 0.979	0.0682 0.0477 0.682 0.7057	

(Continued)

Table 1: Continued

Figure	Panel	Measure	Groups (sample size)	Test	Details	Statistic	p value			
5	D	Effect of secretory IgM on hindlimb swing speed at 4, 8, and 10 weeks post-SCI	8 weeks:	Three-way ANOVA One-way ANOVA for groups within each time point Sidak's multiple comparisons <i>post hoc</i> test on one-way ANOVA Factor 1 (genotype), factor 2 (injury status), factor 3 (time post-SCI)	8 weeks one-way ANOVA KO SCI vs KO sham KO SCI vs WT SCI WT SCI vs WT sham 10 weeks one-way ANOVA KO SCI vs KO sham KO SCI vs WT SCI t = 1.04	F = 3.214	0.0358			
			KO SCI (10),					t = 2.423	0.0624	
			KO sham (8),					t = 2.372	0.0699	
			WT SCI (7),					t = 0.126	0.999	
			WT sham (9) mice					F = 5.733	0.0127	
			10 weeks:							
	KO SCI (9),	t = 3.123	0.0395							
	KO sham (8),	t = 2.474	0.3076							
	WT SCI (6),									
	WT sham (8) mice									
	WT SCI vs WT sham									
	E	Effect of secretory IgM on forelimb swing speed at 4, 8, and 10 weeks post-SCI	Effect of genotype × injury	F = 0.998	0.3205	4 weeks one-way ANOVA KO SCI vs KO sham KO SCI vs WT SCI WT SCI vs WT sham 8 weeks one-way ANOVA KO SCI vs KO sham KO SCI vs WT SCI WT SCI vs WT sham 10 weeks one-way ANOVA KO SCI vs KO sham KO SCI vs WT SCI WT SCI vs WT sham	F = 5.912	0.0024		
4 weeks:										
KO SCI (10),									t = 3.467	0.0044
KO sham (10),									t = 0.139	0.9987
WT SCI (7),									t = 2.337	0.075
WT sham (10) mice										
8 weeks:										
KO SCI (12),									F = 9.014	0.0002
KO sham (8),									t = 4.364	0.0004
WT SCI (7),									t = 0.107	0.9994
WT sham (9) mice										
WT SCI vs WT sham									t = 2.823	0.0242
10 weeks:										
KO SCI (9),	F = 6.61	0.0017								
KO sham (8),	t = 3.418	0.006								
WT SCI (6),	t = 0.777	0.8278								
WT sham (8) mice										
WT SCI vs WT sham	t = 2.595	0.0446								
F	Effect of secretory IgM on hindlimb print area at 4, 8, and 10 weeks post-SCI	Effect of genotype × injury	F = 1.416	0.2371	4 weeks one-way ANOVA KO SCI vs KO sham KO SCI vs WT SCI WT SCI vs WT sham 8 weeks one-way ANOVA KO SCI vs KO sham KO SCI vs WT SCI WT SCI vs WT sham	F = 0.641	0.5941			
								4 weeks:		
								KO SCI (10),	t = 0.239	0.9934
								KO sham (10),	t = 1.082	0.6375
								WT SCI (7),	t = 1.095	0.6291
								WT sham (10) mice		
								8 weeks:		
								KO SCI (12),	F = 1.1	0.3635
								KO sham (8),	t = 0.340	0.9817
								WT SCI (7),	t = 1.393	0.4349
								WT sham (9) mice	t = 0.546	0.9306
								WT SCI vs WT sham	F = 8.787	0.0003

(Continued)

Table 1: Continued

Figure	Panel	Measure	Groups (sample size)	Test	Details	Statistic	p value			
G	Effect of secretory IgM on forelimb print area at 4, 8, and 10 weeks post-SCI		10 weeks:	Three-way ANOVA One-way ANOVA for groups within each time point Sidak's multiple comparisons <i>post hoc</i> test on one-way ANOVA Factor 1 (genotype), factor 2 (injury status), factor 3 (time post-SCI)	10 weeks one-way ANOVA KO SCI vs KO sham KO SCI vs WT SCI WT SCI vs WT sham Effect of genotype × injury	t = 2.31 t = 4.399 t = 0.467 F = 0.676	0.0838 0.0005 0.955 0.4132			
			KO SCI (9),							
			KO sham (8),							
			WT SCI (6),							
			WT sham (8) mice							
			4 weeks:					4 weeks one-way ANOVA	F = 0.927	0.4387
			KO SCI (10),					KO SCI vs KO sham	t = 0.808	0.8098
			KO sham (10),					KO SCI vs WT SCI	t = 0.968	0.7129
			WT SCI (7),					WT SCI vs WT sham	t = 0.526	0.937
			WT sham (10) mice					8 weeks one-way ANOVA	F = 3.558	0.025
			8 weeks:					KO SCI vs KO sham	t = 0.661	0.8846
			KO SCI (12),					KO SCI vs WT SCI	t = 1.111	0.6188
KO sham (8),	WT SCI vs WT sham	t = 3.121	0.0114							
WT SCI (7),	10 weeks one-way ANOVA	F = 7.978	0.0006							
WT sham (9) mice	KO SCI vs KO sham	t = 2.636	0.0406							
10 weeks:	KO SCI vs WT SCI	t = 1.231	0.5416							
KO SCI (9),	WT SCI vs WT sham	t = 3.068	0.0145							
KO sham (8),	Effect of genotype × injury	F = 0.558	0.457							
WT SCI (6),	Three-way ANOVA One-way ANOVA for groups within each time point Sidak's multiple comparisons <i>post hoc</i> test on one-way ANOVA Factor 1 (genotype), factor 2 (injury status), factor 3 (time post-SCI)	Effect of secretory IgM on average body speed at 4, 8, and 10 weeks post-SCI	4 weeks:	4 weeks one-way ANOVA	F = 11.75	< 0.0001				
WT sham (8) mice										
4 weeks:							KO SCI vs KO sham	t = 4.275	0.0005	
KO SCI (10),							KO SCI vs WT SCI	t = 0.757	0.8374	
KO sham (10),							WT SCI vs WT sham	t = 4.099	0.0008	
WT SCI (7),							8 weeks one-way ANOVA	F = 13.56	< 0.0001	
WT sham (10) mice							KO SCI vs KO sham	t = 5.539	< 0.0001	
8 weeks:							KO SCI vs WT SCI	t = 1.353	0.46	
KO SCI (12),							WT SCI vs WT sham	t = 2.87	0.0215	
KO sham (8),							10 weeks one-way ANOVA	F = 10.08	0.0001	
WT SCI (7),							KO SCI vs KO sham	t = 3.972	0.0014	
WT sham (9) mice							KO SCI vs WT SCI	t = 0.678	0.8776	
10 weeks:	WT SCI vs WT sham	t = 3.507	0.0048							
KO SCI (9),										
KO sham (8),										
WT SCI (6),										
WT sham (8) mice										

p values <0.05 are shown in bold for emphasis.

#NB30930) and compared binding of antibodies to untreated sections. However, we did not find a significant difference in binding of anti-C3b antibody between the samples treated with Fc block and the untreated samples, even in sections of high antibody binding such as the injury epicenter (data not shown). Thus, binding of the anti-C3b antibody in our spinal cord sections was not Fc-mediated.

Total levels of circulating IgG were similar between IgM-KO and WT mice at BSL (24 h before SCI) and at 2

and 10 weeks post-SCI (Fig. 1H; Table 1). This suggests that increased presence of parenchymal IgG deposition in IgM-KO mice at two weeks post-SCI is not because of higher circulating IgG levels in these mice. Moreover, IgG levels increased in both groups at 2 and 10 weeks post-SCI compared with their respective BSL levels (Fig. 1H; Table 2). Lastly, while there was no detectable IgM immunoglobulin in KO mice before and after the injury, serum levels of IgM increased at two weeks following SCI (Fig. 1I; Table 2).

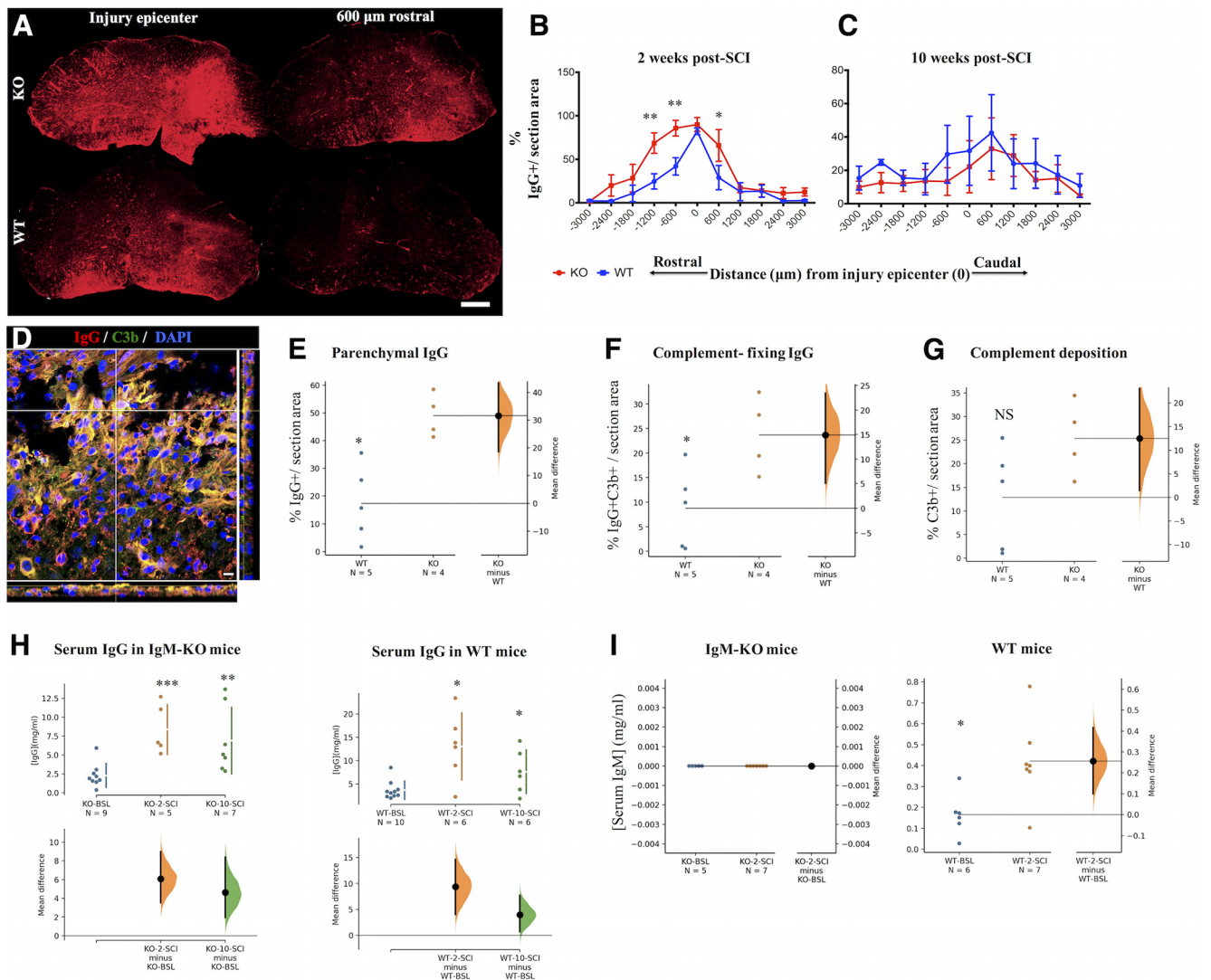


Figure 1. IgM KO mice have more parenchymal IgG antibodies with enhanced complement-fixing activity. **A**, IgG deposition in spinal cord sections of IgM-KO and IgM-WT mice at two weeks post-SCI. Scale bar: 100 μm . **B**, Comparison of the % detected IgG+ immunofluorescent area between groups at two weeks following SCI. See Table 1 for statistics details. **C**, Comparison of the % detected IgG+ immunofluorescent area between groups at 10 weeks following SCI. See Table 1 for statistics details. **D**, Representative section stained for IgG (red) and complement C3b protein (green). Yellow signal indicates co-localization of IgG and C3b. Scale bar: 10 μm . **E–G**, Gardner–Altman estimation plots of % immunofluorescent area from deposited IgG, IgG+C3b, and C3b averaged between sections –1200, –600, and +600 μm from the injury epicenter, and normalized per section area ($N=4–5$ animals/group). See Table 2 for statistics details. **H**, Gardner–Altman estimation plots of total serum IgG levels in IgM-KO and WT mice at BSL (pre-SCI) and at 2 and 10 weeks post-SCI. There is no difference in IgG levels between IgM-KO and WT mice within each time point (data not shown; see statistical Table 1 for details about WT vs KO comparisons). Serum IgG levels increase significantly after injury when compared with their BSL levels in IgM-KO and WT mice. See Table 2 for statistics details. **I**, Gardner–Altman estimation plots of total serum IgM levels in IgM-KO and WT mice at BSL and at two weeks post-SCI, indicating a significant increase of IgM levels in WT mice, following SCI. See Table 2 for statistics details. NS = nonsignificant. Graphs **B**, **C**: mean \pm SEM, * $p < 0.05$, ** $p < 0.01$ (see Table 1 for detailed p values). Graphs **E–I**: permutation t test, * $p < 0.05$, ** $p < 0.01$, *** $p < 0.001$ (see Table 2 for detailed p values).

IgM-KO mice have more T-lymphocytes and microglia/macrophages with myelin-engulfing activity in the lesioned spinal cord

Inflammation mediated by microglia/macrophages and T-lymphocytes is a well-known regulator of pathophysiology in SCI (for review, see Donnelly and Popovich, 2008). Thus, we asked whether the absence of IgM in mice with

SCI was linked to an enhanced presence of T-lymphocytes and microglia/macrophages. Indeed, IgM-KO mice showed larger CD3+ immunofluorescent areas and CD3+ cell counts, as compared with WT controls, at two weeks post-SCI (Fig. 2; Table 1). At 10 weeks post-SCI there was no difference in CD3+ immunofluorescence area between the IgM-KO and WT groups, but IgM-KO

Table 2: Estimation statistics table showing effect size (unpaired means difference) with 95% CIs and permutation tests *p* values as follows: effect size [CI width with lower bound, upper bound]

Figure	Panel	Measure	Groups (sample size)	Effect size [CI width]	Permutation <i>p</i> value		
1	E	Effect of secretory IgM on the % area of IgG deposition at 2 weeks in select sections (–1200, –600, 600 μm).	KO (4 mice, 3 sections each)	31.6 [95%CI 18.6, 43.4]	0.0108		
			WT (5 mice, 3 sections each)				
	F	Effect of secretory IgM on the % area of IgG and C3b co-localization at 2 weeks in select sections (–1200, –600, 600 μm).	KO (4 mice, 3 sections each)	14.9 [95%CI 5.07, 23.4]	0.03		
			WT (5 mice, 3 sections each)				
	G	Effect of secretory IgM on the % area of C3b deposition at 2 weeks in select sections (–1200, –600, 600 μm).	KO (4 mice, 3 sections each)	12.5 [95%CI 1.48, 23.1]	0.116		
			WT (5 mice, 3 sections each)				
	H	Effects of secretory IgM on levels of serum IgG immunoglobulin	KO: BSL (9), 2 weeks (5), 10 weeks (7) mice	KO-2-SCI minus KO-BSL: 6.09 [95%CI 3.51, 8.99] KO-10-SCI minus KO-BSL: 4.62 [95%CI 1.95, 8.39]	0.0004 0.004		
			WT: BSL (10), 2 weeks (6), 10 weeks (6) mice	WT-2-SCI minus WT-BSL: 9.36 [95%CI 4.02, 14.6] WT-10-SCI minus WT-BSL: 3.96 [95%CI 0.703, 7.71]	0.0016 0.0228		
			WT: BSL (6), 2 weeks (7) mice	0.256 [95%CI 0.1, 0.416]	0.0146		
3	E	Effect of secretory IgM on expansion of myelin engulfing macrophages in spinal cord sections with largest IgG deposition.	KO (4 mice, 3 sections each) WT (5 mice, 3 sections each)	4.24 [95%CI 1.07, 7.19]	0.0246		
5	A	Effect of secretory IgM on BMS scores at 2 weeks post-SCI	KO (7), WT (7) mice	–0.286 [95%CI –1.86, 0.643]	0.575		
		Effect of secretory IgM on grip strength at 2 weeks post-SCI	KO (7), WT (7) mice	3.74 [95%CI –6.4, 13.3]	0.485		
5	C	Effect of secretory IgM on step sequence regularity at 4, 8, and 10 weeks post-SCI	4 weeks: KO SCI (10), KO sham (10), WT SCI (7), WT sham (10) mice	KO SCI vs WT SCI –3.95 [95%CI –23.1, 16.8]	0.739		
			8 weeks: KO SCI (10), KO sham (8), WT SCI (7), WT sham (9) mice	KO SCI vs WT SCI –22.5 [95%CI –38.6, –8.21]	0.0196		
			10 weeks: KO SCI (7), KO sham (8), WT SCI (6), WT sham (8) mice	KO SCI vs WT SCI 31.4 [95.0%CI –49.4, –12.2]	0.0188		
			D	Effect of secretory IgM on hindlimb swing speed at 4, 8, and 10 weeks post-SCI	4 weeks: KO SCI (10), KO sham (10), WT SCI (7), WT sham (10) mice	KO SCI vs WT SCI –7.22 [95%CI –20.9, 4.97]	0.358
					8 weeks: KO SCI (12), KO sham (8),	KO SCI vs WT SCI –16.1 [95%CI –34.6, –4.95]	0.0598

(Continued)

Table 2: Continued

Figure	Panel	Measure	Groups (sample size)	Effect size [CI width]	Permutation <i>p</i> value		
5	E	Effect of secretory IgM on forelimb swing speed at 4, 8, and 10 weeks post-SCI	WT SCI (7), WT sham (9) mice	KO SCI vs WT SCI -18.2 [95%CI -32.9, -3.69]	0.0412		
			10 weeks: KO SCI (9), KO sham (8), WT SCI (6), WT sham (8) mice				
			4 weeks: KO SCI (10), KO sham (10), WT SCI (7), WT sham (10) mice			KO SCI vs WT SCI 0.859 [95%CI -11.3, 12.7]	0.896
			8 weeks: KO SCI (12), KO sham (8), WT SCI (7), WT sham (9) mice			KO SCI vs WT SCI -0.507 [95%CI -8.66, 9.56]	0.925
			10 weeks: KO SCI (9), KO sham (8), WT SCI (6), WT sham (8) mice			KO SCI vs WT SCI -4.87 [95.0%CI -20.5, 7.37]	0.524
			4 weeks: KO SCI (10), KO sham (10), WT SCI (7), WT sham (10) mice			KO SCI vs WT SCI -0.0616 [95%CI -0.175, 0.08]	0.425
	F	Effect of secretory IgM on hindlimb print area at 4, 8, and 10 weeks post-SCI	8 weeks: KO SCI (12), KO sham (8), WT SCI (7), WT sham (9) mice	KO SCI vs WT SCI -0.037[95%CI -0.0826, 0.024]	0.289.		
			10 weeks: KO SCI (9), KO sham (8), WT SCI (6), WT sham (8) mice	KO SCI vs WT SCI -0.096 [95%CI -0.137, -0.0501]	0.0006		
			4 weeks: KO SCI (10), KO sham (10), WT SCI (7), WT sham (10) mice	KO SCI vs WT SCI -0.0352 [95%CI -0.115, 0.0438]	0.43		
			8 weeks: KO SCI (12), KO sham (8), WT SCI (7), WT sham (9) mice	KO SCI vs WT SCI 0.0192 [95%CI -0.0109, 0.055]	0.352		
			10 weeks: KO SCI (9), KO sham (8), WT SCI (6), WT sham (8) mice	KO SCI vs WT SCI -0.023 [95%CI -0.0664, 0.0159]	0.35		
			4 weeks: KO SCI (10), KO sham (10), WT SCI (7), WT sham (10) mice	KO SCI vs WT SCI 2.39 [95%CI -2.51, 8.17]	0.424		
G	Effect of secretory IgM on hindlimb print area at 4, 8, and 10 weeks post-SCI	8 weeks: KO SCI (12), KO sham (8), WT SCI (7), WT sham (9) mice	KO SCI vs WT SCI -3.52 [95%CI -7.53, 1.42]	0.171			
		10 weeks: KO SCI (9), KO sham (8), WT SCI (6), WT sham (8) mice	KO SCI vs WT SCI -3.52 [95%CI -7.53, 1.42]	0.171			
		4 weeks: KO SCI (10), KO sham (10), WT SCI (7), WT sham (10) mice	KO SCI vs WT SCI 2.39 [95%CI -2.51, 8.17]	0.424			
		8 weeks: KO SCI (12), KO sham (8), WT SCI (7), WT sham (9) mice	KO SCI vs WT SCI 0.0192 [95%CI -0.0109, 0.055]	0.352			
		10 weeks: KO SCI (9), KO sham (8), WT SCI (6), WT sham (8) mice	KO SCI vs WT SCI -0.023 [95%CI -0.0664, 0.0159]	0.35			
		4 weeks: KO SCI (10), KO sham (10), WT SCI (7), WT sham (10) mice	KO SCI vs WT SCI -0.0352 [95%CI -0.115, 0.0438]	0.43			
H	Effect of secretory IgM on average body speed at 4, 8, and 10 weeks post-SCI	8 weeks: KO SCI (12), KO sham (8), WT SCI (7), WT sham (9) mice	KO SCI vs WT SCI -0.037[95%CI -0.0826, 0.024]	0.289.			
		10 weeks: KO SCI (9), KO sham (8), WT SCI (6), WT sham (8) mice	KO SCI vs WT SCI -0.096 [95%CI -0.137, -0.0501]	0.0006			
		4 weeks: KO SCI (10), KO sham (10), WT SCI (7), WT sham (10) mice	KO SCI vs WT SCI -0.0616 [95%CI -0.175, 0.08]	0.425			
		8 weeks: KO SCI (12), KO sham (8), WT SCI (7), WT sham (9) mice	KO SCI vs WT SCI -0.507 [95%CI -8.66, 9.56]	0.925			
		10 weeks: KO SCI (9), KO sham (8), WT SCI (6), WT sham (8) mice	KO SCI vs WT SCI -4.87 [95.0%CI -20.5, 7.37]	0.524			
		4 weeks: KO SCI (10), KO sham (10), WT SCI (7), WT sham (10) mice	KO SCI vs WT SCI -0.0616 [95%CI -0.175, 0.08]	0.425			

(Continued)

Table 2: Continued

Figure	Panel	Measure	Groups (sample size)	Effect size [CI width]	Permutation <i>p</i> value
			10 weeks: KO SCI (9), KO sham (8), WT SCI (6), WT sham (8) mice	KO SCI vs WT SCI −2.31 [95%CI −8.24, 3.55]	0.49
6	B	Effect of secretory IgM on bacterial load in bladder at 2 weeks post-SCI	KO (7), WT (7) mice	0.429 [95%CI 0.0, 1.29]	0
	C	Effect of secretory IgM on bacterial load in colon at 2 weeks post-SCI	KO (7), WT (6) mice Upon log-transformation:	1.29e+02 [95%CI −2.01e+02, 7e+02]	0.877
	D	Effect of secretory IgM on body weight at 2 weeks post-SCI	KO (5), WT (6) mice KO (7), WT (7) mice	−1.54 [95%CI −7.52, 3.85]	0.617
	E	Effect of secretory IgM on spleen weight at 2 weeks post-SCI	KO (7), WT (7) mice	0.005 [95%CI −0.0206, 0.0272]	0.686

p values for permutation tests <0.05 are shown in bold for emphasis.

mice showed elevated CD3+ cell counts overall, and especially 1800 μ m rostrally from the injury epicenter (Fig. 2C; Table 1).

In line with our hypothesis, we also found significantly larger CD11b+ %immunostained areas in IgM-KO mice than in WT mice at 2 weeks but not at 10 weeks (Fig. 3A, B; Table 1) of SCI. CD11b+ cell counts were higher in IgM-KO mice at both 2 and 10 weeks after injury (Fig. 3C; Table 1).

Next, we asked whether these microglia/macrophages had engulfed myelin, and whether there was a difference between IgM-KO mice and WT mice regarding the extent of myelin engulfment by microglia/macrophages. To this end, we semi-quantified the %area that was co-stained for CD11b and fluoromyelin (Fig. 3D) in sections with the highest IgG deposition (i.e., −1200, −600, and +600 μ m from the injury epicenter) at two weeks post-SCI. Our data showed a significant increase in CD11b+fluoromyelin+ areas in the spinal cords of IgM-KO mice compared with WT controls at two weeks of SCI (Fig. 3E; Table 2), suggesting enhanced myelin engulfment by microglia/macrophages in the absence of IgM immunoglobulin.

IgM-KO mice have larger lesion size in comparison to WT mice following SCI

We quantified the volume of lesional tissue and white/gray matter sparing at 2 and 10 weeks post-SCI. Lesioned areas were present in both the gray and the white matter. In the gray matter, lesions had inflammation, apparent disruption of the normal cytoarchitecture along with fibrosis. In the white matter, lesions presented with inflammation, loss of LFB staining and vacuoles (Fig. 4A). There was no statistical difference between the groups in the volumes of lesional tissue (Fig. 4B; Table 1) or white matter preservation (Fig. 4C; Table 1) at two weeks of injury. However, the preserved gray matter was significantly lower in IgM KO mice, particularly at 600 μ m rostral from the injury epicenter (Fig. 4D; Table 1).

Of note, IgM KO mice had significant loss of neural tissue at 10 weeks post-SCI. Compared with their WT counterparts, IgM-KO mice with SCI had more lesional tissue,

especially rostral to the injury epicenter (Fig. 4E; Table 1). Concomitantly, IgM-KO mice had less white matter preservation rostrally and caudally from the injury epicenter (Fig. 4F; Table 1), while both groups had similar gray matter preservation (Fig. 4G; Table 1) at 10 weeks after injury.

IgM deficiency results in impaired locomotor recovery during the chronic phase of SCI

At two weeks post-SCI, IgM-KO mice and their WT counterparts showed similar locomotor and grip strength performance in BMS and grip strength tests, respectively (Fig. 5A; Table 2). However, at later time points, IgM-KO mice with SCI had impaired coordination and hindlimb function compared with their WT counterparts, based on their performance on the CatWalk test (Fig. 5B). In particular, injured KO mice had worse interlimb coordination compared with WT mice at 8 and 10 weeks post-SCI, as indicated by lower % step sequence regularity indices [Fig. 5C; Table 1 (for multiple comparisons across all time points and groups); Table 2 (for estimation statistics comparing WT-SCI to KO-SCI at each time point)]. By 10 weeks of injury, the difference between IgM-KO and WT mice with SCI was striking, with the regularity index ranging between 44–88% in WT mice, and 14–65% in KO mice.

Hindlimb swing speed was significantly impaired in KO mice compared with WT at 10 weeks of injury [Fig. 5D; Table 1 (for multiple comparisons across all time points and groups); Table 2 (for estimation statistics comparing WT-SCI to KO-SCI at each time point)]. Forelimb swing speed was significantly decreased in both genotypes after SCI when compared with their sham counterparts (Fig. 5E; Table 1). However, the absence of IgM did not appear to affect forelimb swing speed, as injured WT and IgM-KO mice showed similar recovery (Fig. 5E; Table 2).

IgM-KO mice had significantly smaller hindlimb print areas than their WT counterparts at 10 weeks after injury (Fig. 5F; Table 2). In both genotype groups, forelimb print area was reduced after injury when compared with their sham counterparts (Fig. 5G; Table 1). However, there was

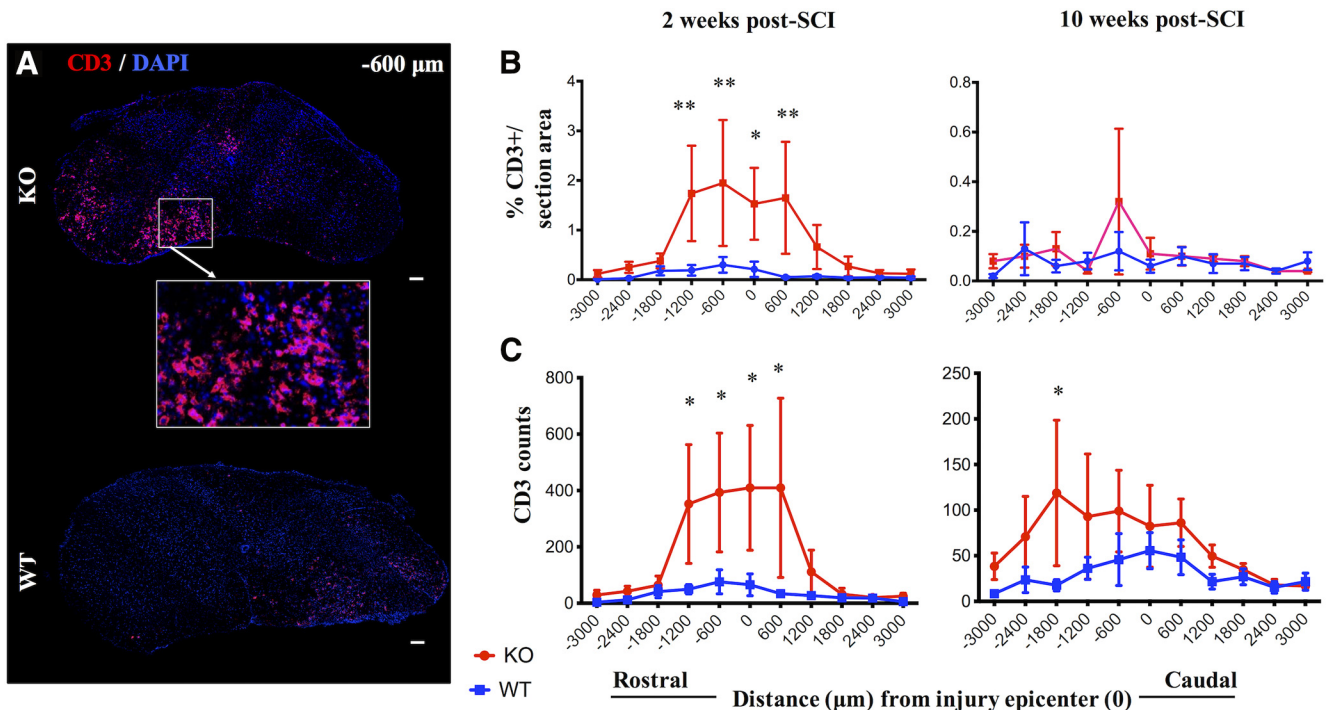


Figure 2. IgM-KO mice have increased T-lymphocyte infiltration compared with WT mice at two weeks post-SCI. **A**, Representative sections stained for T-lymphocytes marker CD3 and DAPI in IgM-KO and WT mice at two weeks post-SCI. Quantification of % CD3+ immunostained area/total spinal cord section area (**B**) and CD3 cell counts (**C**) rostral-caudally from the injury epicenter, at 2 and 10 weeks post-injury in IgM-KO and WT mice. $N=4-5$ mice/group (**B**), 5 mice/group (**C**), mean \pm SEM; * $p < 0.05$, ** $p < 0.01$ (see Table 1 for detailed statistical results).

no difference in forelimb print areas between IgM-KO and WT mice with SCI (Fig. 5G; Table 2). Despite the above differences in coordination, hindlimb swing speed and hindlimb print area between the IgM-KO and WT mice with SCI, the average body speed was similar between IgM-KO and WT mice at all time points of the study [Fig. 5H; Table 1 (for multiple comparisons across all time points and groups); Table 2 (for estimation statistics comparing WT-SCI to KO-SCI at each time point)].

IgM deficiency does not result in respiratory tract infections or urinary tract infections (UTIs)

Infections have been shown to negatively affect neurologic recovery in SCI (Failli et al., 2012). Respiratory tract infections and UTIs are common complications in patients with SCI (Garcia-Arguello et al., 2017). As the peripheral immune response is particularly suppressed during the subacute phase of C7/T1 SCI in rats (Uldreaj et al., 2017), we hypothesized that IgM-KO mice would have increased bacteria in their bladders and signs of pneumonia in their lungs at two weeks post-SCI. To test this hypothesis, we quantified the bacterial load in bladders of IgM-KO and WT mice with SCI and assessed for signs of inflammation in the lungs (e.g., abnormal presence of macrophages, increased numbers of macrophages and abnormal tissue structure) at two weeks after injury. There were no signs of lung inflammation in IgM-KO mice compared with WT mice (Fig. 6A). In addition, we found no significant increase in bacterial counts in the bladders of IgM-KO mice compared with WT mice

with SCI (Fig. 6B; Table 2). Similar microbial counts were found in gut cultures (isolated from the colon), which were used as a positive control for detection and culturing of bacteria (Fig. 6C; Table 2). Other important metrics of recovery from SCI (Brommer et al., 2016) such as body weight (Fig. 6D; Table 2) and spleen weight (Fig. 6E; Table 2) were also similar between IgM-KO and WT mice at two weeks after injury.

Discussion

This study shows that deficiency of IgM immunoglobulin results in impaired recovery following cervical SCI in mice. Overall, IgM-KO mice exhibited worse neurobehavioral recovery, coupled with increased lesion size, less white matter sparing, and enhanced deposition of complement-fixing IgG antibodies in the spinal cord as compared with their WT counterparts. These data provide evidence for the necessary role of IgM immunoglobulin in spontaneous recovery during cervical SCI and warrant further research into the therapeutic effect of IgM administration after SCI. A recent clinical trial showing significant benefits of IgM-enriched immunoglobulin preparation for patients with pneumonia and lower levels of endogenous IgM (Brunner et al., 2013; Cavazzuti et al., 2014; Wand et al., 2016; Welte et al., 2018; Kalvelage et al., 2019; Willuweit et al., 2019) further supports this notion.

Using a rat model of cervical SCI, we previously found early extravasation of IgM immunoglobulin in the lesioned spinal cord and a chronic expansion of splenic IgM

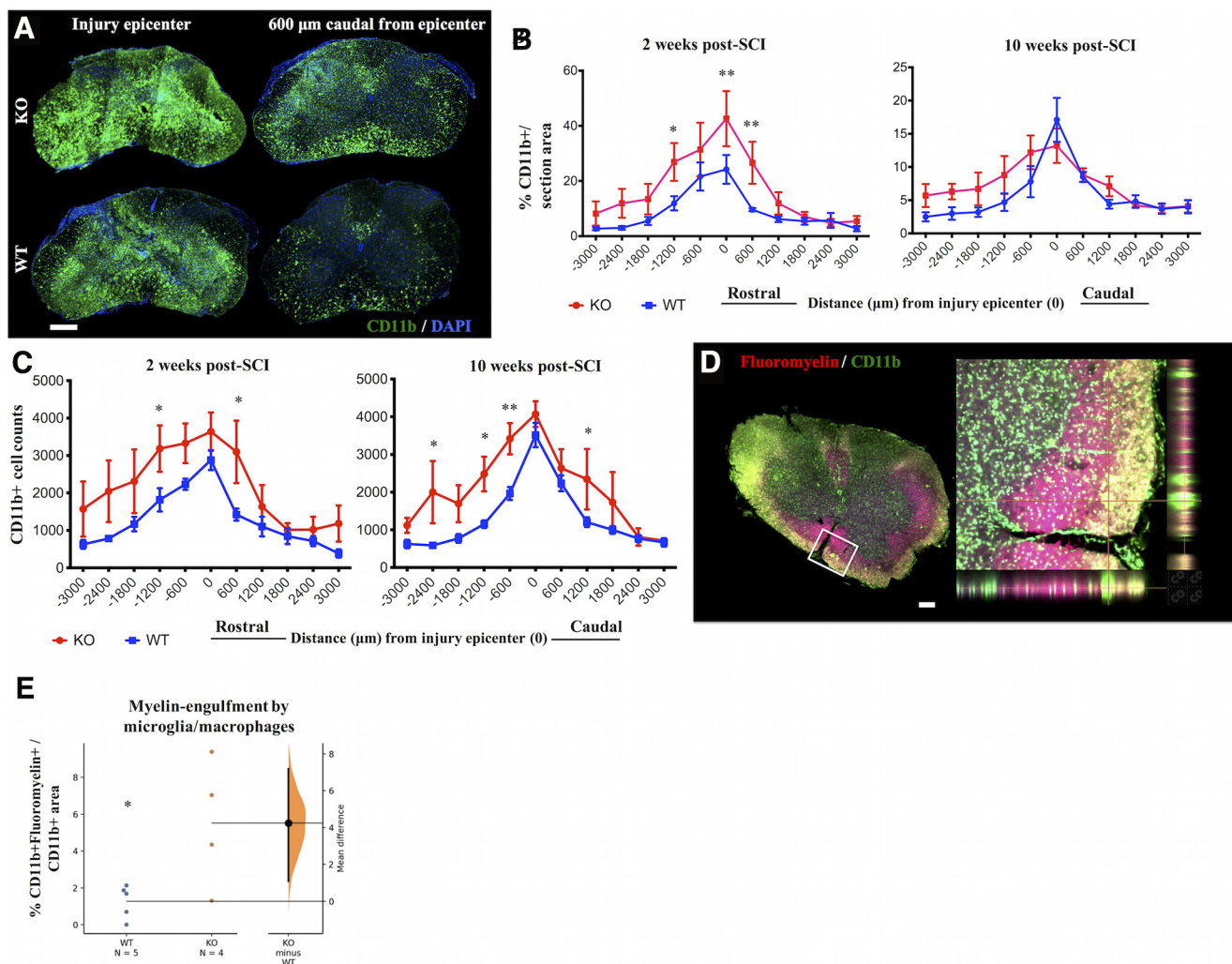


Figure 3. IgM-KO mice have more microglia/macrophages than WT controls. **A**, Representative spinal cord sections stained for the microglia/macrophage markers CD11b and DAPI at two weeks post-SCI. Quantification of % CD11b+ immunostained areas/total area (**B**) and CD11b+ cell counts (**C**) rostro-caudally from the injury epicenter, at 2 and 10 weeks of injury. **D**, Representative spinal cord section stained for myelin (fluoromyelin) and microglia/macrophages (CD11b) at two weeks post-SCI. Inset indicates area of co-localized CD11b and fluoromyelin signal. Myelin-engulfing macrophages appear yellow because of colocalization of green (CD11b+ signal) and red (fluoromyelin) signals in the single layer confocal image. **E**, Gardner-Altman estimation plot showing quantification of % area of co-localized CD11b+ and fluoromyelin+ signal/total section area. Each dot indicates mean as averaged from 3 sections/animal, where sections were taken at distances -1200 , -600 , and $+600$ μm from the injury epicenter. Scale bar: 100 μm , $N = 4$ – 5 animals/group (**B**, **E**), 5 animals/group (**C**). Error bars indicate SEM; * $p < 0.05$, ** $p < 0.01$. See Table 1 for detailed statistical results in **B**, **C** and Table 2 for statistical results in **E**.

plasma cells (UIndreaj et al., 2017). Additionally, we have observed chronically increased levels of serum IgM immunoglobulin in rats after cervical SCI (UIndreaj et al., 2020). Circulating IgM immunoglobulin comprises the majority of naturally occurring antibodies. By binding a broad range of self and non-self-targets, naturally occurring antibodies constitute a rapid innate response to altered self-antigens and invading pathogens, thereby maintaining homeostasis against autoimmunity, infectious and other diseases (Ehrenstein and Notley, 2010). Thus, we hypothesized that the enhanced IgM response we observed in our rat SCI model could be protective. To test this hypothesis we induced C6/C7 SCI in mice that lack secretory IgM immunoglobulin (Boes et al., 1998b) and

compared their outcomes to WT littermate controls. These IgM-KO mice have undetectable serum IgM, although they express membrane IgM and all other secretory immunoglobulin classes (Boes et al., 1998b).

IgM-KO mice had significant deficits in coordination and other gait parameters in their hindlimbs compared with their WT counterparts during the chronic time points of our study (8–10 weeks post-SCI). When compared with shams, mice with SCI showed overall impairment in coordination, swing speed and print area in both fore- and hindlimbs, thus confirming the impairments previously observed in our C6/C7 SCI mouse model (Forgione et al., 2017). When comparing IgM-KO to WT mice with SCI, KO mice had greater impairments in coordination, lowered

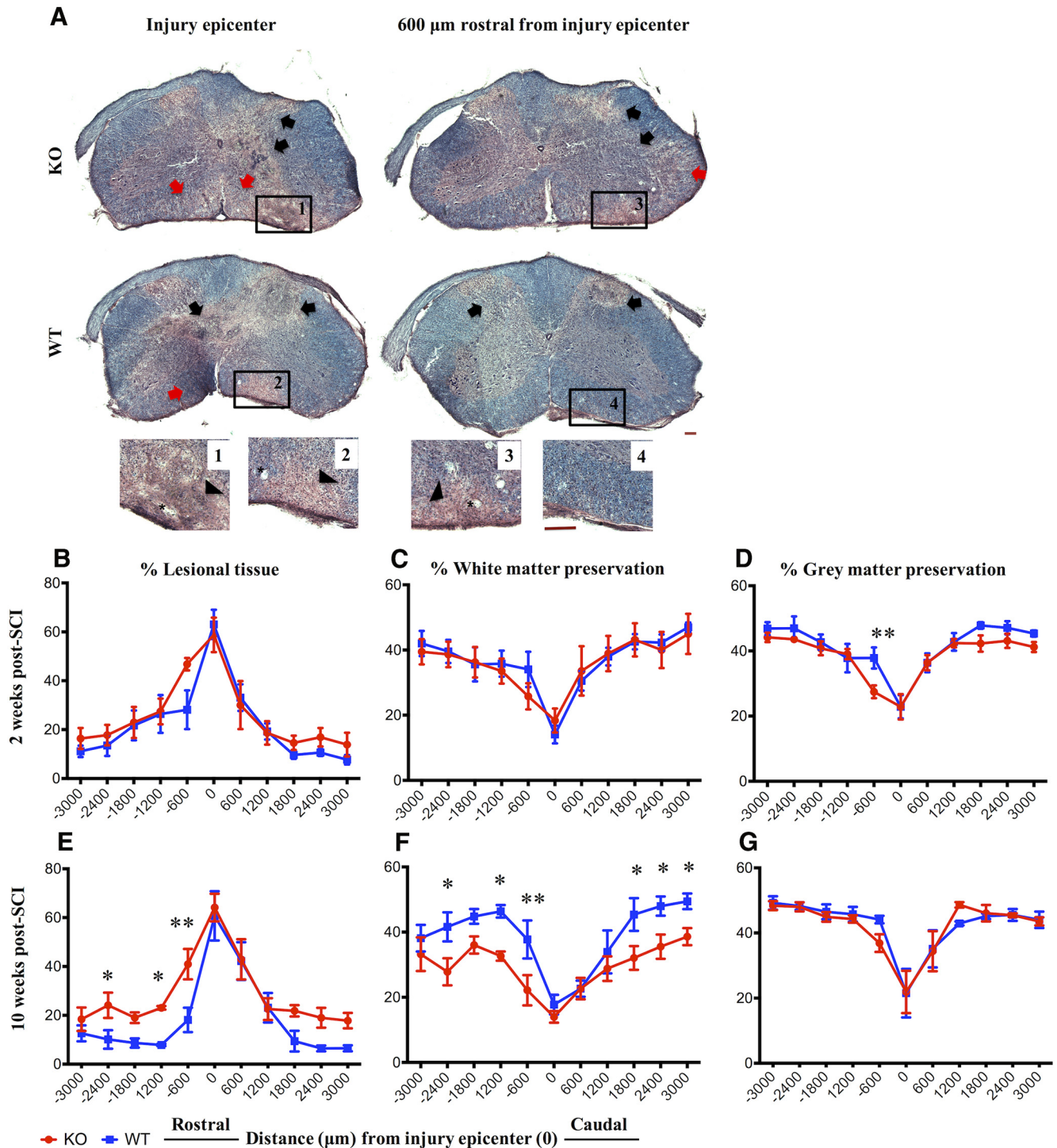


Figure 4. IgM KO mice have more lesional tissue at 10 weeks post-SCI. **A**, Representative HE and LFB images of spinal cord cross-sections taken from an injured IgM-KO and WT mouse at the injury epicenter and 600 μm rostral from the injury epicenter at 10 weeks post-SCI. Insets 1–4 indicate most severe lesional tissue. Black arrows indicate gray matter lesions and red arrows indicate white matter lesions. Asterisks indicate vacuoles. Scale bar: 100 μm. **B–G**, Quantification of lesional tissue and white/gray matter preservation by the Cavalieri method at 2 and 10 weeks post-SCI rostral-caudally from the injury epicenter. **B–D**, Lesional tissue and white and gray matter preservation in IgM-KO and WT mice at two weeks of injury. **E–G**, Lesional tissue and white and gray matter preservation at 10 weeks of injury $N = 4–5$ /group; mean \pm SEM; * $p < 0.05$, ** $p < 0.01$.

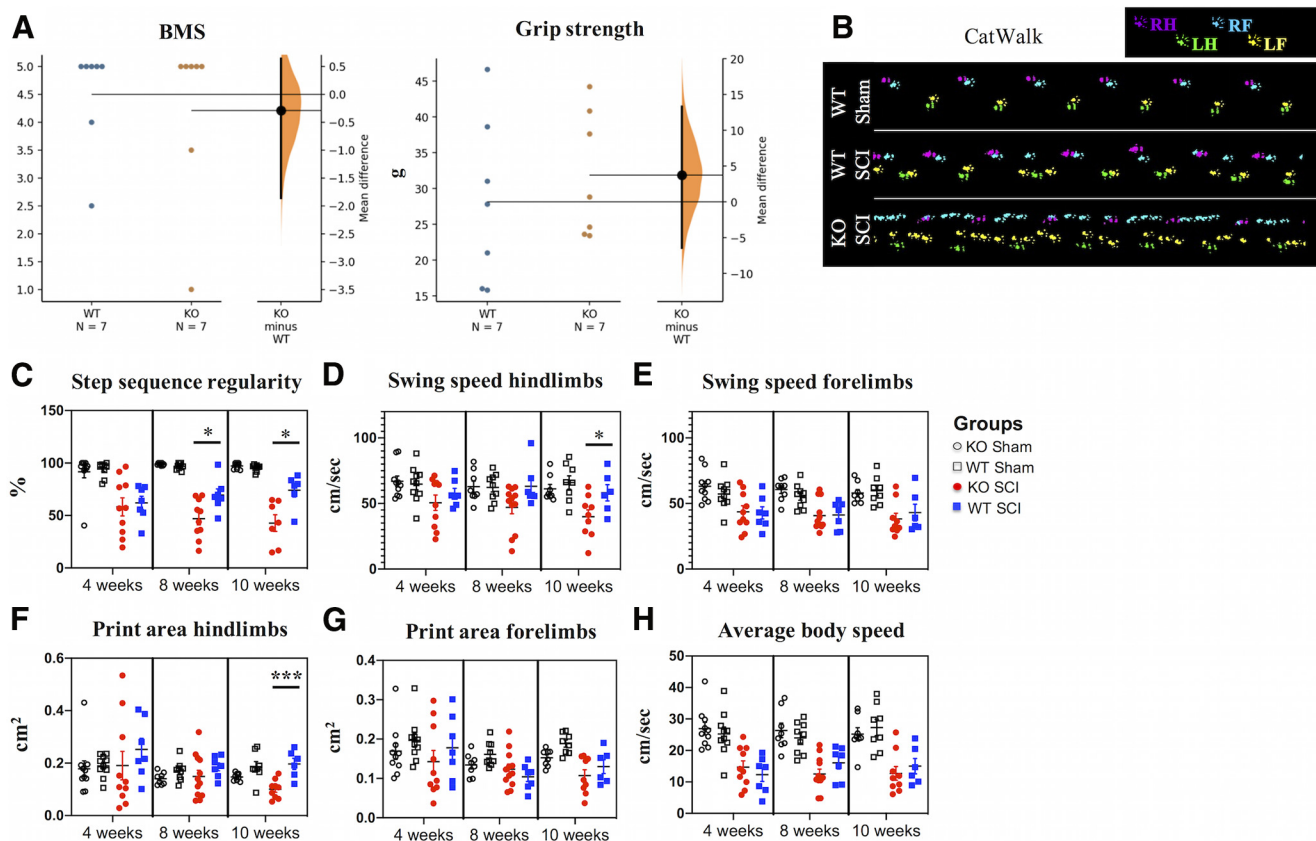


Figure 5. IgM deficiency results in impaired coordination during the chronic phase of SCI. **A**, Gardner–Altman estimation plots of BMS and grip strength scores at two weeks after injury. See [Table 2](#) for statistics details. **B**, Representative images of locomotion in a sham WT animal as well as a WT and KO mouse with SCI at 10 weeks after injury, as recorded with CatWalk. **C**, IgM-KO mice with SCI show deteriorated coordination compared with injured WT mice, as indicated by smaller step sequence regularity indices at 8 and 10 weeks after injury. See [Table 2](#) for statistics details between WT and KO mice. **D**, Hindlimb swing speed is slower in IgM-KO mice with SCI compared with their WT counterparts at 10 weeks of injury ([Table 2](#)). **E**, There is no difference between WT and KO mice with SCI in forelimb swing speed ([Table 2](#)). **F**, Hindlimb print area is significantly smaller in KO mice with SCI, compared with their WT counterparts ([Table 2](#)). **G**, Forelimb print areas are similar between IgM-KO and WT mice with SCI ([Table 2](#)). **H**, Average body speed is similar between IgM-KO and WT mice with SCI ([Table 2](#)). Group size: $N=6-12$ mice/group. Mean \pm SEM, * $p < 0.05$, *** $p < 0.001$. Only significant differences between WT SCI and KO SCI groups are indicated with * on the graph, based on results shown in [Table 2](#). For details on statistical analyses considering the effect of genotype, time after injury, and injury status on parameters shown in **C–H**, see [Table 1](#).

swing speed and smaller print area in the hindlimbs. Importantly, both groups had similar average body speeds, suggesting that the above differences did not result from the confounding effect of body speed ([Batka et al., 2014](#)).

In line with these chronic neurologic impairments, we found increased lesion size and less white matter sparing in IgM-KO mice compared with WT mice at our last chronic time point of the study (10 weeks after injury). Interestingly, both groups had similar neurobehavioral and histologic outcomes at two weeks of injury. This suggested that IgM deficiency may affect pathomechanisms that are initiated during or after the two-week time point, which marks the beginning of the subacute phase in rodent SCI.

One relevant mechanism explored here is the expansion of T cells and microglia/macrophages in the injured spinal cord. CD3 and CD11b cell expansion was assessed by quantifying the percent positive immunofluorescent area

and by cell counts in spinal cord sections across a selected rostral-caudal axis from the injury epicenter. Of note, while microglia/macrophage responses are considered to peak by two weeks post-SCI in mice, this time point marks only the onset of T-cell infiltration in the lesioned spinal cord ([Sroga et al., 2003](#)). Also, in patients with SCI T-cell infiltrates are limited in the spinal cord and do not appear until weeks to months after trauma ([Fleming et al., 2006](#)). Given the decline in T-cell signal at 10 weeks, it is possible that here we have missed the peak of T-cell infiltration in the spinal cord. Despite this limitation regarding the optimal time point for the detection of CD3, our data show that compared with WT mice, IgM-KO mice had increased % CD3+ and % CD11b+ immunofluorescence area at two weeks post-SCI. At 10 weeks post-SCI, both groups had similar CD3 and CD11b + immunofluorescence areas. Interestingly, CD3 and CD11b cell counts were significantly higher in IgM-KO mice at both 2 and 10 weeks post-SCI. Our finding of higher CD3 and CD11b cell

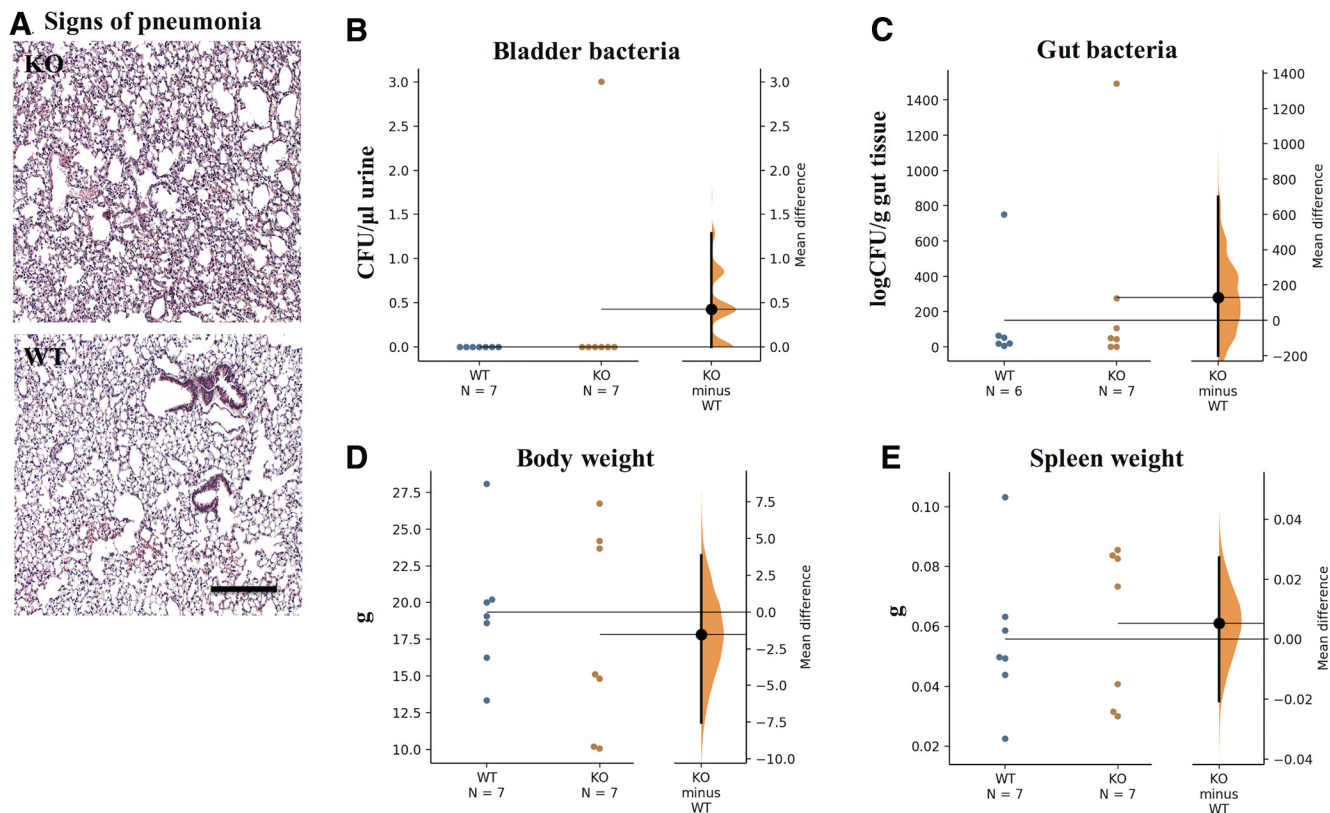


Figure 6. There is no evidence of bladder infection or pneumonia in IgM-KO mice or WT controls at two weeks of SCI. **A**, HE-stained lungs at 4× magnification indicating absence of inflammation. **B**, **C**, Gardner–Altman estimation plots of bladder-bacterial and gut-bacterial load in IgM-KO and WT mice at two weeks of SCI. **D**, **E**, Gardner–Altman estimation plots of body weight (**D**) and spleen weight (**E**) in IgM-KO and WT mice at two weeks post-SCI. CFU = colony forming units; NS = nonsignificant. See [Table 2](#) for detailed statistical results.

counts in IgM-KO mice with similar total immunofluorescence areas as WT mice at 10 weeks suggests that these cells in IgM-KO mice are on average smaller than in WT mice. This in turn can indirectly provide some information on the activation status of such cells or their subtype. For example, while both microglia and blood-derived macrophages are CD11b+, microglia tend to have a larger surface than blood-derived macrophages (Servet-Delprat et al., 2002). Similarly, IgM KO and WT mice may have different composition of CD3 cell subpopulations (CD4, CD8) with varying cell sizes depending on their activation state (Li and Kurlander, 2010). Taken together, these data show that CD3 and CD11b cells are expanded in the spinal cord of IgM-KO mice compared with their WT counterparts and further suggest that the composition of these cells is likely different between IgM-KO and WT mice.

Moreover, we found that IgM-KO mice had increased IgG antibody deposition in the lesioned spinal cord at two weeks of injury. We and others have previously observed extensive widespread IgG in the lesioned parenchyma in SCI models (Ankeny et al., 2009; Uldreaj et al., 2017; Zhou et al., 2019). Such antibodies are localized with neurons (Uldreaj et al., 2017), bind to astrocytes or astrocytic markers (Uldreaj et al., 2017; Arevalo-Martin et al., 2018; Hergenroeder et al., 2018) or to vascular endothelial

cells within the injured spinal cord parenchyma (Zhou et al., 2019). The deposited antibodies can be autoreactive [e.g., IgGs bind to spinal cord components through their F(ab)₂ portion] or not (e.g., IgGs bind to spinal cord cells through their Fc portion), and can persist throughout the disease course (Ankeny et al., 2009) or peak only during the subacute phase of SCI (Uldreaj et al., 2017; Zhou et al., 2019). Regardless, there is strong evidence that IgG deposition in the spinal cord is detrimental to recovery after SCI (Ankeny et al., 2009; Zhou et al., 2019). Of note, circulating levels of IgG were similar between IgM-KO and WT mice at all time points of the study. This suggests that increased parenchymal IgG deposition at two weeks post-SCI in IgM-KO mice is likely not because of higher circulating IgG immunoglobulin. Rather, factors that affect IgG extravasation in the tissue [such as blood-spinal cord barrier (BSCB) disruption] and/or turnover are likely to contribute to enhanced IgG deposition in IgM-KO mice at two weeks post-SCI. The potential effect of IgM on BSCB integrity was outside the scope of this study. However, the accumulation of IgG, which appeared largely in areas mostly affected by the physical impact of clip compression (i.e., injury epicenter, anterior and lateral white matter), suggests that the degree of BSCB disruption may be different between IgM-KO and WT mice.

Here, we do not present direct evidence for the binding specificity of the IgG that was detected in the spinal cord. However, in our previous study we showed that circulating antibodies from rats with cervical SCI bind more strongly to cultured astrocytes (a cell type we found was IgG positive in injured spinal cords) than antibodies from uninjured rats. We also found that the spleen mounts a stronger antibody response against spinal cord antigens after injury. Furthermore, we performed competition assays to show that the signal we detect on the spinal cord is specific (Ulndreaj et al., 2017). These indirect lines of evidence suggest that some of the serum antibodies in mice with SCI are specific to spinal cord antigens. Others have also shown that SCI results in the induction of self-reacting antibodies (Ankeny et al., 2006, 2009). It should be noted that these induced antibodies comprise the minority of circulating antibodies (in the range of $\mu\text{g/ml}$) and we do not think that the signal we see in the spinal cord results exclusively from induced antibodies. Rather, given the large signal detected, we think it represents binding of naturally occurring antibodies that comprise the majority of the antibody pool in the body (in the mg/ml range), and typically bind to self-antigens with low affinity (Lutz, 2007). Such antibodies are elevated following SCI (Arevalo-Martin et al., 2018). Moreover, it has been shown that in the absence of circulating IgM immunoglobulins, there are more self-reacting IgG antibodies (Boes et al., 2000). Taken together, we think the deposition of IgGs in the injured spinal cord in the present study results from at least three non-mutually exclusive phenomena: (1) the BSCB disruption which allows for serum IgGs to enter the parenchyma non-specifically; (2) the binding of naturally occurring antibodies to spinal cord self-antigens with low affinity; (3) the generation of immune auto-IgGs following SCI and potential exacerbation of this response because of the absence of secretory IgM (Boes et al., 2000) specifically.

The histology and inflammation data taken together indicate that enhanced neuroinflammation (rather than worse lesion) during the subacute phase (two weeks post-SCI) is linked to chronic neurobehavioral impairments in IgM-KO mice. This observation is in line with multiple studies linking early neuroinflammation to deteriorated histologic and locomotor outcomes in the chronic phase (Bao et al., 2011; Nguyen et al., 2012; Brennan et al., 2015). It is unclear why IgM-KO and WT mice have similar lesion size at two weeks despite significant differences in neuroinflammation at the same time point. However, a plausible explanation could be that the enhanced inflammation we observed in IgM-KO mice has long-term functional effects that have not been established by two weeks after injury. These effects could be related to processes including regeneration and plasticity (Ballermann and Fouad, 2006; Courtine et al., 2008; Rossignol and Frigon, 2011), and a favorable balance of remyelination/demyelination (Hesp et al., 2015). Such mechanisms, although initiated early on during SCI, take longer to establish and to give rise to quantifiable differences in neurobehavioral outcomes.

One of the mechanisms by which deposited IgGs have been shown to negatively impact outcomes after SCI is through activation of the complement system (Ankeny et al., 2009). In turn, complement activation enhances immune cell infiltration/activation (such as microglia/macrophages and T-lymphocytes; Ankeny et al., 2009; Brennan et al., 2015) and promotes degradation of spared tissue by phagocytosis (Ankeny et al., 2009) or by direct complement-mediated attack (Qiao et al., 2010). Here, we examined whether increased IgG deposition in IgM-KO mice led to enhanced complement fixation in the lesioned spinal cord. In line with this hypothesis, we found enhanced C3b-IgG co-localization in the spinal cord of IgM-KO mice, as compared with their WT counterparts. Interestingly, C3b opsonizes antigens that are further taken up and engulfed by phagocytic cells (such as microglia and macrophages) through the interaction of C3b and complement receptor 3 (CR3), consisting of CD11b and CD18 (Ricklin et al., 2010). In an effort to understand the source of increased myelin loss in IgM-KO mice with SCI, and given the widespread presence of CD11b⁺ cells (typically microglia/macrophages) at two weeks of injury in KO mice, we further hypothesized that myelin was engulfed by CD11b⁺ microglia/macrophages in IgM-KO mice. Indeed, by quantifying the CD11b⁺/fluoromyelin⁺ area in sections with maximum IgG deposition (shown to have increased C3b deposition), we found that IgM-KO mice had significantly more myelin-engulfing microglia/macrophages than their WT counterparts. Taken together, this line of evidence indicates that the absence of secretory IgM immunoglobulin is associated with increased complement-fixing IgGs on the lesioned spinal cord, as well as the widespread presence of myelin-engulfing microglia/macrophages.

Research indicates that secretory IgM protects against detrimental IgG autoimmunity in multiple potentially overlapping pathways, which range from regulating the development of IgG autoantibodies to directly inhibiting their effector functions. For example, IgM antibodies enhance the phagocytic clearance of apoptotic cells and other cellular debris (Chen et al., 2009), which if left uncleared, could trigger pathogenic autoimmune responses (Henson, 2017). In addition, IgM regulates the development of pathogenic IgG autoantibody responses by controlling the generation of autoreactive B cells throughout their life span. Such mechanisms include central tolerance to self-antigens early during B cell development (Nguyen et al., 2015), and later on the reduction of autoreactive BCR signaling (Tsiantoulas et al., 2017) and deletion/deactivation of self-reactive B cells (Ouchida et al., 2012). Moreover, IgM immunoglobulin inhibits IgG autoantibody effector functions by binding directly to IgG's F(ab')₂ component, thereby inhibiting IgG binding to self-antigens (Adib et al., 1990). We tested the latter possibility, given that in a previous study we found significant deposition of IgM antibodies in the spinal cord following C7 SCI in rats (Ulndreaj et al., 2017). However, contrary to our rat data, we did not find any significant IgM deposition at 2 or 10 weeks of injury in injured WT mice (data not shown), suggesting that IgM does not inhibit IgG binding in the injured spinal cord.

Of note, IgM's protective effects on SCI recovery could be independent of IgG. For example, IgM was shown to induce proliferation of oligodendrocyte-precursor cells (OPCs) via $Fc\alpha/\mu R$ signaling during brain development (Tanabe and Yamashita, 2018). Occurring within the first two weeks post-SCI, and primarily rostrally from the injury epicenter (Li and Leung, 2015), oligodendrogenesis is an endogenous regenerative process in rodent SCI (Zai and Wrathall, 2005; Lytle and Wrathall, 2007; Tripathi and McTigue, 2007; Lytle et al., 2009; Li and Leung, 2015) and has been a therapeutic target for multiple research groups aiming to reverse myelin loss after injury (Karimi-Abdolrezaee et al., 2006; Plemel et al., 2014; Papastefanaki and Matsas, 2015). Thus, future studies could investigate whether secretory IgM promotes endogenous OPC proliferation in SCI.

Importantly, circulating IgM is the carrier and regulator of AIM (also known as CD5L/Spalpha/API6; Hiramoto et al., 2018), a protein with debris clearance and macrophage survival function. In the absence of secretory IgM, circulating levels of AIM are undetectable and insufficient debris clearance was shown to lead to worsened disease progression in a model of acute kidney injury (Arai and Miyazaki, 2018). It is thus possible that worse outcomes observed in IgM-KO mice with SCI in the present study are because of insufficient AIM-mediated debris clearance. This possibility should be explored in future studies as AIM was shown to be a top gene upregulated by microglia/macrophages after SCI (Zhu et al., 2017), yet its role in SCI remains unknown.

In addition to the above positive effects, IgM protects against microbial infections. Here, we looked at a possible link between IgM deficiency and microbial infections after injury, as infections are linked with poor neurologic recovery in SCI (Failli et al., 2012; Brommer et al., 2016) and IgM-KO mice have been shown to be susceptible to microbial infections in past studies (Baumgarth et al., 2005). As UTIs and pneumonia are the most frequent infection types in patients with SCI (Garcia-Arguello et al., 2017), we looked at microbial loads in the bladder and signs of inflammation in the lungs at two weeks after injury. However, we found no signs of bladder infection or lung inflammation. Thus, our data suggest that the impaired recovery after SCI in the absence of secretory IgM immunoglobulin is not because of infections. However, it is important to note that our experiments were conducted in mice that were receiving antibiotics in their water and were infection free.

Although our data suggest that total IgM immunoglobulin may have a protective role in SCI, it is important to note that not all IgM is beneficial for SCI. For example, some natural IgM antibodies were shown to have significant detrimental effects on SCI outcomes by activating the immune system and further enhancing secondary injury (Narang et al., 2017). This duality of the IgM response during SCI reflects the overall complex role of the immune response in SCI pathophysiology, which has made the journey to discovering effective SCI therapies challenging. Delineating the role of critical pathophysiological factors in SCI recovery, such as important components of the

immune system, will take us closer to developing effective treatments for this debilitating chronic condition, which given its complex nature, will ultimately necessitate the application of an array of treatment modalities (Ulndreaj et al., 2016).

In conclusion, the present study shows that IgM immunoglobulin is important for recovery following cervical SCI, as IgM deficiency resulted in impaired neurobehavioral and histologic outcomes, as well as increased IgG deposition, complement activation, T- cell infiltration and myelin-engulfing macrophages. We anticipate that future research will investigate whether circulating IgM levels are useful biomarkers of recovery in patients with SCI, and ultimately, whether modulating IgM immunoglobulin levels can improve recovery.

References

- Adib M, Ragimbeau J, Avrameas S, Ternynck T (1990) IgG autoantibody activity in normal mouse serum is controlled by IgM. *J Immunol* 145:3807–3813.
- Ankeny DP, Lucin KM, Sanders VM, McGaughy VM, Popovich PG (2006) Spinal cord injury triggers systemic autoimmunity: evidence for chronic B lymphocyte activation and lupus-like autoantibody synthesis. *J Neurochem* 99:1073–1087.
- Ankeny DP, Guan Z, Popovich PG (2009) B cells produce pathogenic antibodies and impair recovery after spinal cord injury in mice. *J Clin Invest* 119:2990–2999.
- Arai S, Miyazaki T (2018) A scavenging system against internal pathogens promoted by the circulating protein apoptosis inhibitor of macrophage (AIM). *Semin Immunopathol* 40:567–575.
- Arevalo-Martin A, Grassner L, Garcia-Ovejero D, Paniagua-Torija B, Barroso-Garcia G, Arandilla AG, Mach O, Turrero A, Vargas E, Alcobendas M, Rosell C, Alcaraz MA, Ceruelo S, Casado R, Talavera F, Palazón R, Sanchez-Blanco N, Maier D, Esclarin A, Molina-Holgado E (2018) Elevated autoantibodies in subacute human spinal cord injury are naturally occurring antibodies. *Front Immunol* 9:2365.
- Ballermann M, Fouad K (2006) Spontaneous locomotor recovery in spinal cord injured rats is accompanied by anatomical plasticity of reticulospinal fibers. *Eur J Neurosci* 23:1988–1996.
- Bao F, Fleming JC, Golshani R, Pearse DD, Kasabov L, Brown A, Weaver LC (2011) A selective phosphodiesterase-4 inhibitor reduces leukocyte infiltration, oxidative processes, and tissue damage after spinal cord injury. *J Neurotrauma* 28:1035–1049.
- Basso DM, Fisher LC, Anderson AJ, Jakeman LB, McTigue DM, Popovich PG (2006) Basso mouse scale for locomotion detects differences in recovery after spinal cord injury in five common mouse strains. *J Neurotrauma* 23:635–659.
- Batka RJ, Brown TJ, Mcmillan KP, Meadows RM, Jones KJ, Haulcomb MM (2014) The need for speed in rodent locomotion analyses. *Anat Rec (Hoboken)* 297:1839–1864.
- Baumgarth N, Herman OC, Jager GC, Brown LE, Herzenberg LA, Chen J (2000) B-1 and B-2 cell-derived immunoglobulin M antibodies are nonredundant components of the protective response to influenza virus infection. *J Exp Med* 192:271–280.
- Baumgarth N, Tung JW, Herzenberg LA (2005) Inherent specificities in natural antibodies: a key to immune defense against pathogen invasion. *Springer Semin Immunopathol* 26:347–362.
- Boes M, Prodeus AP, Schmidt T, Carroll MC, Chen J (1998a) A critical role of natural immunoglobulin M in immediate defense against systemic bacterial infection. *J Exp Med* 188:2381–2386.
- Boes M, Esau C, Fischer MB, Schmidt T, Carroll M, Chen J (1998b) Enhanced B-1 cell development, but impaired IgG antibody responses in mice deficient in secreted IgM. *J Immunol* 160:4776–4787.

- Boes M, Schmidt T, Linkemann K, Beaudette BC, Marshak-Rothstein A, Chen J (2000) Accelerated development of IgG autoantibodies and autoimmune disease in the absence of secreted IgM. *Proc Natl Acad Sci USA* 97:1184–1189.
- Brennan FH, Gordon R, Lao HW, Biggins PJ, Taylor SM, Franklin RJM, Woodruff TM, Ruitenberg MJ (2015) The complement receptor C5aR controls acute inflammation and astrogliosis following spinal cord injury. *J Neurosci* 35:6517–6531.
- Brommer B, Engel O, Kopp MA, Watzlawick R, Müller S, Prüss H, Chen Y, DeVivo MJ, Finkenstaedt FW, Dirnagl U, Liebscher T, Meisel A, Schwab JM (2016) Spinal cord injury-induced immune deficiency syndrome enhances infection susceptibility dependent on lesion level. *Brain* 139:692–707.
- Brunner R, Rinner W, Haberler C, Kitzberger R, Sycha T, Herkner H, Warszawska J, Madl C, Holzinger U (2013) Early treatment with IgM-enriched intravenous immunoglobulin does not mitigate critical illness polyneuropathy and/or myopathy in patients with multiple organ failure and SIRS/sepsis: a prospective, randomized, placebo-controlled, double-blinded trial. *Crit Care* 17:R213.
- Cavazzuti I, Serafini G, Busani S, Rinaldi L, Biagioni E, Buoncrisiano M, Girardis M (2014) Early therapy with IgM-enriched polyclonal immunoglobulin in patients with septic shock. *Intensive Care Med* 40:1888–1896.
- Chen Y, Park YB, Patel E, Silverman GJ (2009) IgM antibodies to apoptosis-associated determinants recruit C1q and enhance dendritic cell phagocytosis of apoptotic cells. *J Immunol* 182:6031–6043.
- Courtine G, Song B, Roy RR, Zhong H, Herrmann JE, Ao Y, Qi J, Edgerton VR, Sofroniew MV (2008) Recovery of supraspinal control of stepping via indirect propriospinal relay connections after spinal cord injury. *Nat Med* 14:69–74.
- Davies AL, Hayes KC, Dekaban GA (2007) Clinical correlates of elevated serum concentrations of cytokines and autoantibodies in patients with spinal cord injury. *Arch Phys Med Rehabil* 88:1384–1393.
- DeVivo MJ, Krause JS, Lammertse DP (1999) Recent trends in mortality and causes of death among persons with spinal cord injury. *Arch Phys Med Rehabil* 80:1411–1419.
- Donnelly DJ, Popovich PG (2008) Inflammation and its role in neuroprotection, axonal regeneration and functional recovery after spinal cord injury. *Exp Neurol* 209:378–388.
- Ehrenstein MR, Notley CA (2010) The importance of natural IgM: scavenger, protector and regulator. *Nat Rev Immunol* 10:778–786.
- Failli V, Kopp MA, Gericke C, Martus P, Klingbeil S, Brommer B, Laginha I, Chen Y, DeVivo MJ, Dirnagl U, Schwab JM (2012) Functional neurological recovery after spinal cord injury is impaired in patients with infections. *Brain* 135:3238–3250.
- Fleming JC, Norenberg MD, Ramsay DA, Dekaban GA, Marcillo AE, Saenz AD, Pasquale-Styles M, Dietrich WD, Weaver LC (2006) The cellular inflammatory response in human spinal cords after injury. *Brain* 129:3249–3269.
- Förger F, Matthias T, Oppermann M, Becker H, Helmke K (2004) Clinical significance of anti-dsDNA antibody isotypes: IgG/IgM ratio of anti-dsDNA antibodies as a prognostic marker for lupus nephritis. *Lupus* 13:36–44.
- Forgione N, Chamankhah M, Fehlings MG (2017) A mouse model of bilateral cervical contusion-compression spinal cord injury. *J Neurotrauma* 34:1227–1239.
- García-Arguello LY, O'Horo JC, Farrell A, Blakney R, Sohail MR, Evans CT, Safdar N (2017) Infections in the spinal cord-injured population: a systematic review. *Spinal Cord* 55:526–534.
- Hayes KC, Hull TCL, Delaney GA, Potter PJ, Sequeira KAJ, Campbell K, Popovich PG (2002) Elevated serum titers of proinflammatory cytokines and CNS autoantibodies in patients with chronic spinal cord injury. *J Neurotrauma* 19:753–761.
- Henson PM (2017) Cell removal: efferocytosis. *Annu Rev Cell Dev Biol* 33:127–144.
- Hergenroeder GW, Redell JB, Choi HA, Schmitt L, Donovan W, Francisco GE, Schmitt K, Moore AN, Dash PK (2018) Increased levels of circulating glial fibrillary acidic protein and collapsin response mediator protein-2 autoantibodies in the acute stage of spinal cord injury predict the subsequent development of neuropathic pain. *J Neurotrauma* 35:2530–2539.
- Hesp ZC, Goldstein EZ, Goldstein EA, Miranda CJ, Kaspar BK, Kaspar BK, McTigue DM (2015) Chronic oligodendrogenesis and remyelination after spinal cord injury in mice and rats. *J Neurosci* 35:1274–1290.
- Hiramoto E, Tsutsumi A, Suzuki R, Matsuoka S, Arai S, Kikkawa M, Miyazaki T (2018) The IgM pentamer is an asymmetric pentagon with an open groove that binds the AIM protein. *Sci Adv* 4:eaau1199.
- Ho J, Tumkaya T, Aryal S, Choi H, Claridge-Chang A (2019) Moving beyond P values: data analysis with estimation graphics. *Nat Methods* 16:565–566.
- Kalvelage C, Zacharowski K, Bauhofer A, Gockel U, Adamzik M, Nierhaus A, Kujath P, Eckmann C, Pletz MW, Bracht H, Simon TP, Winkler M, Kindgen-Milles D, Albertsmeier M, Weigand M, Ellger B, Ragaller M, Ullrich R, Marx G (2019) Personalized medicine with IgGAM compared with standard of care for treatment of peritonitis after infectious source control (the PEPPER trial): study protocol for a randomized controlled trial. *Trials* 20:156.
- Karimi-Abdolrezaee S, Eftekharpour E, Wang J, Morshead CM, Fehlings MG (2006) Delayed transplantation of adult neural precursor cells promotes remyelination and functional neurological recovery after spinal cord injury. *J Neurosci* 26:3377–3389.
- Kopp MA, Watzlawick R, Martus P, Failli V, Finkenstaedt FW, Chen Y, DeVivo MJ, Dirnagl U, Schwab JM (2017) Long-term functional outcome in patients with acquired infections after acute spinal cord injury. *Neurology* 88:892–900.
- Li N, Leung GKK (2015) Oligodendrocyte precursor cells in spinal cord injury: a review and update. *BioMed Res Int* 2015:235195.
- Li Y, Kurlander RJ (2010) Comparison of anti-CD3 and anti-CD28-coated beads with soluble anti-CD3 for expanding human T cells: differing impact on CD8 T cell phenotype and responsiveness to restimulation. *J Transl Med* 8:104.
- Lutz HU (2007) Homeostatic roles of naturally occurring antibodies: an overview. *J Autoimmun* 29:287–294.
- Lytle JM, Wrathall JR (2007) Glial cell loss, proliferation and replacement in the contused murine spinal cord. *Eur J Neurosci* 25:1711–1724.
- Lytle JM, Chittajallu R, Wrathall JR, Gallo V (2009) NG2 cell response in the CNP-EGFP mouse after contusive spinal cord injury. *Glia* 57:270–285.
- Miyazaki T, Yamazaki T, Sugisawa R, Gershwin ME, Arai S (2018) AIM associated with the IgM pentamer: attackers on stand-by at aircraft carrier. *Cell Mol Immunol* 15:563–574.
- Mizrachi Y, Ohry A, Aviel A, Rozin R, Brooks ME, Schwartz M (1983) Systemic humoral factors participating in the course of spinal cord injury. *Paraplegia* 21:287–293.
- Narang A, Qiao F, Atkinson C, Zhu H, Yang X, Kulik L, Holers VM, Tomlinson S (2017) Natural IgM antibodies that bind neoepitopes exposed as a result of spinal cord injury, drive secondary injury by activating complement. *J Neuroinflammation* 14:120.
- Nguyen DH, Cho N, Satkunendrarajah K, Austin JW, Wang J, Fehlings MG (2012) Immunoglobulin G (IgG) attenuates neuroinflammation and improves neurobehavioral recovery after cervical spinal cord injury. *J Neuroinflammation* 9:224.
- Nguyen TTT, Elsner RA, Baumgarth N (2015) Natural IgM prevents autoimmunity by enforcing B cell central tolerance induction. *J Immunol* 194:1489–1502.
- Ouchida R, Mori H, Hase K, Takatsu H, Kurosaki T, Tokuhisa T, Ohno H, Wang JY (2012) Critical role of the IgM Fc receptor in IgM homeostasis, B-cell survival, and humoral immune responses. *Proc Natl Acad Sci USA* 109:E2699–E2706.
- Papastefanaki F, Matsas R (2015) From demyelination to remyelination: the road toward therapies for spinal cord injury. *Glia* 63:1101–1125.
- Petrova NV, Ponomaryova AM, Alyoshkin VA, Elisseyev AT, Yumashev GS (1993) Serum rheumatoid factors in spinal cord injury patients. *Paraplegia* 31:265–268.

- Plemel JR, Keough MB, Duncan GJ, Sparling JS, Yong VW, Stys PK, Tetzlaff W (2014) Remyelination after spinal cord injury: is it a target for repair? *Prog Neurobiol* 117:54–72.
- Qiao F, Atkinson C, Kindy MS, Shunmugavel A, Morgan BP, Song H, Tomlinson S (2010) The alternative and terminal pathways of complement mediate post-traumatic spinal cord inflammation and injury. *Am J Pathol* 177:3061–3070.
- Ricklin D, Hajishengallis G, Yang K, Lambris JD (2010) Complement: a key system for immune surveillance and homeostasis. *Nat Immunol* 11:785–797.
- Rossignol S, Frigon A (2011) Recovery of locomotion after spinal cord injury: some facts and mechanisms. *Annu Rev Neurosci* 34:413–440.
- Sanjurjo L, Amézaga N, Aran G, Naranjo-Gómez M, Arias L, Armengol C, Borràs FE, Sarrias M-R (2015) The human CD5L/ALM-CD36 axis: a novel autophagy inducer in macrophages that modulates inflammatory responses. *Autophagy* 11:487–502.
- Servet-Delprat C, Arnaud S, Jurdic P, Nataf S, Grasset MF, Soulas C, Domenget C, Destaing O, Rivollier A, Perret M, Dumontel C, Hanau D, Gilmore GL, Belin MF, Rabourdin-Combe C, Mouchiroud G (2002) FIt3+ macrophage precursors commit sequentially to osteoclasts, dendritic cells and microglia. *BMC Immunol* 3:15.
- Sroga JM, Jones TB, Kigerl KA, McGaughy VM, Popovich PG (2003) Rats and mice exhibit distinct inflammatory reactions after spinal cord injury. *J Comp Neurol* 462:223–240.
- Su J, Georgiades A, Wu R, Thulin T, de Faire U, Frostegård J (2006) Antibodies of IgM subclass to phosphorylcholine and oxidized LDL are protective factors for atherosclerosis in patients with hypertension. *Atherosclerosis* 188:160–166.
- Tanabe S, Yamashita T (2018) B-1a lymphocytes promote oligodendrogenesis during brain development. *Nat Neurosci* 21:506–516.
- Tripathi R, McTigue DM (2007) Prominent oligodendrocyte genesis along the border of spinal contusion lesions. *Glia* 55:698–711.
- Tsiantoulas D, Kiss M, Bartolini-Gritti B, Bergthaler A, Mallat Z, Jumaa H, Binder CJ (2017) Secreted IgM deficiency leads to increased BCR signaling that results in abnormal splenic B cell development. *Sci Rep* 7:3540.
- Uldreaj A, Chio JCT, Ahuja CS, Fehlings MG (2016) Modulating the immune response in spinal cord injury. *Expert Rev Neurother* 16:1127–1129.
- Uldreaj A, Tzekou A, Mothe AJ, Siddiqui AM, Dragas R, Tator CH, Torlakovic EE, Fehlings MG (2017) Characterization of the antibody response after cervical spinal cord injury. *J Neurotrauma* 34:1209–1226.
- Uldreaj A, Tzekou A, Siddiqui AM, Fehlings MG (2020) Effects of experimental cervical spinal cord injury on peripheral adaptive immunity. *PLoS One* 15:e0241285.
- Vidal PM, Karadimas SK, Uldreaj A, Laliberte AM, Tetreault L, Forner S, Wang J, Foltz WD, Fehlings MG (2017) Delayed decompression exacerbates ischemia-reperfusion injury in cervical compressive myelopathy. *JCI Insight* 2:e92512.
- Wand S, Klages M, Kirbach C, Warszawska J, Meybohm P, Zacharowski K, Koch A (2016) IgM-enriched immunoglobulin attenuates systemic endotoxin activity in early severe sepsis: a before-after cohort study. *PLoS One* 11:e0160907.
- Welte T, Dellinger RP, Ebel H, Ferrer M, Opal SM, Singer M, Vincent JL, Werdan K, Martin-Loeches I, Almirall J, Artigas A, Ignacio Ayestarán J, Nuding S, Ferrer R, Sirgo Rodríguez G, Shankar-Hari M, Álvarez-Lerma F, Riessen R, Sirvent JM, Kluge S, et al. (2018) Efficacy and safety of trimodulin, a novel polyclonal antibody preparation, in patients with severe community-acquired pneumonia: a randomized, placebo-controlled, double-blind, multicenter, phase II trial (CIGMA study). *Intensive Care Med* 44:438–448.
- Willuweit K, Bezinover D, Herzer K, Nowak KM, Paul A, Saner FH (2019) Efficacy of IgM-enriched immunoglobulin for vasopressor-resistant vasoplegic shock after liver transplantation. *Transplantation* 103:381–386.
- Zai LJ, Wrathall JR (2005) Cell proliferation and replacement following contusive spinal cord injury. *Glia* 50:247–257.
- Zajarías-Fainsod D, Carrillo-Ruiz J, Mestre H, Grijalva I, Madrazo I, Ibarra A (2012) Autoreactivity against myelin basic protein in patients with chronic paraplegia. *Eur Spine J* 21:964–970.
- Zhou T, Zheng Y, Sun L, Badea SR, Jin Y, Liu Y, Rolfe AJ, Sun H, Wang X, Cheng Z, Huang Z, Zhao N, Sun X, Li J, Fan J, Lee C, Megraw TL, Wu W, Wang G, Ren Y (2019) Microvascular endothelial cells engulf myelin debris and promote macrophage recruitment and fibrosis after neural injury. *Nat Neurosci* 22:421–435.
- Zhu Y, Lyapichev K, Lee DH, Motti D, Ferraro NM, Zhang Y, Yahn S, Soderblom C, Zha J, Bethea JR, Spiller KL, Lemmon VP, Lee JK (2017) Macrophage transcriptional profile identifies lipid catabolic pathways that can be therapeutically targeted after spinal cord injury. *J Neurosci* 37:2362–2376.